CZECH TECHNICAL UNIVERSITY IN PRAGUE

FACULTY OF MECHANICAL ENGINEERING

Department of Process Engineering

CFD simulation of heat transfer in an agitated vessel with a pitched six-blade turbine impeller

Master thesis

Gokul Sai Namburi

Name of the supervisor: Ing Karel Petera, Ph.D.

MASTER'S THESIS ASSIGNMENT

I. Personal and study details

Student's name: **Namburi Gokul Sai** Personal ID number: **453500**

Faculty / Institute: **Faculty of Mechanical Engineering**

Department / Institute: **Department of Process Engineering**

Study program: **Mechanical Engineering**

Branch of study: **Process Engineering**

II. Master's thesis details

Master's thesis title in English:

CFD simulation of heat transfer in an agitated vessel with a pitched six-blade turbine impeller

Master's thesis title in Czech:

CFD simulation of heat transfer in an agitated vessel with a pitched six-blade turbine impeller

Guidelines:

- Make a literature research concerning the heat transfer in agitated vessels.
- Create a model for the given geometry in ANSYS CFD.
- Perform numerical simulations of heat transfer in the agitated vessel for different rotation speeds and evaluate heat transfer coefficients at the bottom and vertical wall.
- Evaluate the impact of the impeller distance from the bottom.
- Summarize the methodology used in the thesis and propose possible improvements of the solution procedure.

Bibliography / sources:

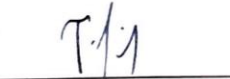Name and workplace of master's thesis supervisor:

Ing. Karel Petera, Ph.D.,   Department of Process Engineering,   FME
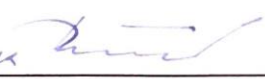
Name and workplace of second master's thesis supervisor or consultant:

Date of master's thesis assignment: **23.10.2018**   Deadline for master's thesis submission: **11.01.2019**

Assignment valid until: _____

_____
Ing. Karel Petera, Ph.D.
Supervisor's signature

_____
prof. Ing. Tomáš Jirout, Ph.D.
Head of department's signature

_____
prof. Ing. Michael Valášek, DrSc.
Dean's signature

III. Assignment receipt

The student acknowledges that the master's thesis is an individual work. The student must produce his thesis without the assistance of others, with the exception of provided consultations. Within the master's thesis, the author must state the names of consultants and include a list of references.

_30.10.2018_
Date of assignment receipt

_____
Student's signature

I.   Personal Details

Student's name:	Namburi Gokul Sai
Personal ID number:	453500
Faculty:	Faculty of Mechanical Engineering
Department:	Department of Process Engineering
Study program:	Mechanical Engineering
Branch of study:	Process Engineering

II.   Master's thesis details

Master's thesis title in English

CFD simulation of heat transfer in an agitated vessel with pitched six-blade turbine impeller

Supervisor's name: Doc. Ing. Karel Petera, Ph.D.

III.   Content of the supplement

The defense of the thesis was performed on 12th February, 2019. The result of the defense based on the committee decision was that the student was classified by grade F - failed. Due to this fact the committee recommended to arrange and correct the thesis according to specified requirements. The exact record of the committee evaluation is stated in the RECORD OF THE FINAL STATE EXAMINATION from 12th February, 2019.

IV.   Recommended improvement and objectives extension

The committee recommended to rewrite the thesis with emphasis to improvement of formal aspects of thesis which were negatively evaluated by reviewer. The objectives extension is not required. It is also possible to concern the improvement of the poor technical aspects of the thesis pointed out by reviewer.
1. Rewrite the text to improve the language level.
2. Improve the citation and reference list in the text.

V.   Important dates

Date of master's thesis supplement assignment: 15.2.2019
Deadline for corrected master's thesis submission: 7.6.2019

doc. Ing. Karel Petera, Ph.D.	Prof. Ing. Tomáš Jirout, Ph.D.	Prof. Ing. Michael Valášek, DrSc.
Supervisor's signature	Head of department's signature	Dean's signature

VI.   Supplement Assignment receipt

The student acknowledges that the master's thesis is an individual work. The student must produce his thesis without the assistance of others, with the exception of provided consultations. Within the master's thesis, the author must state the names of consultants and include a list of references.

15 -02- 2019

Date of assignment receipt

Student signature

<u>Declaration</u>

I hereby declare that I have completed this thesis entitled **CFD Simulation of Heat Transfer in an Agitated Vessel with a Pitched Six-Blade Turbine Impeller** independently with consultations with my supervisor and I have attached a full list of used reference and citations.

I do not have a compelling reason against the use of the thesis within the meaning of Section 60 of the Act No.121/2000 Coll., on copyright, rights related to copyright and amending some laws (Copyright Act).

In …. Prague…, Date: Name: ………………

ACKNOWLEDGEMENT

ABSTRACT

In this work, heat transfer to a Newtonian fluid in a jacketed vessel equipped with a pitched blade turbine (PBT) has been numerically investigated. The turbine has six blades at a 45^0 angle and it is placed in a cylindrically baffled vessel with a flat top and bottom. The cylindrical walls and bottom of the vessel are maintained at constant heat flux q = 3000 W/m^2 boundary condition. Numerical simulations of heat transfer in the agitated vessel for different rotational speeds from 300 to 900 rpm were performed. Heat transfer coefficients at the bottom and vertical walls with off-bottom clearance h/d =1, 2/3, 1/3 (impeller distance from the bottom of the agitated vessel) were evaluated. To study the flow field and transient heat transfer in the agitated vessel, a commercial software ANSYS Fluent 15.0 has been employed. The sliding mesh technique available in ANSYS Fluent was used to model flow around the rotating impeller. k-ω based Shear-Stress-Transport (SST) turbulence model was chosen to model turbulence. An internal source (sink) of heat was used to eliminate the increase of fluid temperature, which might influence the evaluation of the heat transfer coefficients. By performing the transient simulations, the Nusselt numbers at the bottom, wall and bottom + wall were evaluated, and the heat transfer correlation was developed and compared with experimental data in the existing literature.

Keywords: CFD, transient heat transfer simulation, PBT, heat sink, off-bottom clearance, sliding mesh, Nusselt number.

Table of Contents

CHAPTER 1 INTRODUCTION AND OBJECTIVES

1.1 Introduction

In many chemical industries and processing units, mixing liquids, solid-liquid suspensions, gas-liquid dispersions, etc., plays an important role. For these applications, agitated vessels are used in industries like food, pharmaceutical, water treatment plants, manufacture of paints and cosmetics, etc. In fact, these two-words, agitation and mixing have different meaning. Agitation refers to forcing a fluid by mechanical equipment to flow in a circulatory or other pattern inside a closed container. Mixing is a random distribution of two different or the same phases of fluids. A good example of the agitated vessel used in food processing industry is to maintain homogeneity of milk which has to be well mixed to prevent the milk fat from creaming. Temperature control and uniform distribution in order to slow down or prevent the growth of bacteria and is necessary yeast, fresh milk needs be chilled to and kept at a certain temperature during storage (Brodkey et al., 1998).

In process industries agitation promotes an excellent example of occurring homogenizing of temperature, physical properties, chemical reactions, heat transfer, mass transfer of components. Mixing leads to good quality of products and homogeneity of materials.

Agitation vessel is furnished with the tank, impeller mounted on an overhung shaft, baffles in contact with the process fluid and accessories such as inlet, outlet lines, drain valve and coils, jackets providing the heating system. The design of agitated vessel varies widely depending on the application in industrial scale model or experimental work in laboratory scale up. In the following chapters about, agitated vessel parameters and theory are briefly explained.

Heat transfer in an agitated vessel is one of the most important factors to be considered for maintaining the quality of the product. Usually, the agitated vessel has heat transfer surface in form of a jacket or internal coil, for supplying or removing heat from the vessel. A recirculation loop with an external heat exchanger can be used. Depending on the fluid in the agitated vessel heat transfer rate is set. Dimensionless groups are frequently used to express relation between mixing intensity and heat transfer.

Process engineering mainly focuses on design, operations, and maintenance of equipment in chemical and manufacturing industries. Process engineer role is to fill the gap in between recovery of raw material and manufacturing of final products. Process engineer must apply

the key concepts of mechanical and fluid dynamics principles to the conversion of matter by the effect of mechanical action. Process engineering benefits significantly from modelling and simulation as a mean to optimize existing processes and design new once and to overcome the drawback of old models. To fulfil the above tasks, computational fluid dynamics (CFD) helps to analyze the design and modelling of fluid flows in the geometry. Due to the complexity of the fluid flows, CFD further helps to visualize and determine the fluid pattern, heat transfer, velocity profiles of the design. In recent years there is vast upgrade in technology, which helps to design the model and test it with real-time conditions to save the investment cost and production cost (Brenner, 2009).

1.2 Objectives

1. Study and design a model of agitated vessel geometry by using ANSYS Design Modeler, numerical simulations are to perform with software ANSYS 15.0 version.

2. Numerical simulations of heat transfer in an agitated vessel for different rotation speeds between 300 to 900 rpm (in specific 300, 400, 500, 600, 700, 800, 900 rpm) and constant heat flux source of q= 3000 W/m^2 at the bottom as well as at the vertical walls of the vessel. For one of the cases at rotational speed of 500 rpm, to perform simulation at constant heat flux of q= 30000 W/m^2 and to compare the heat transfer results with the simulation performed at constant heat flux source of q= 3000 W/m^2.

3. Evaluate the impact of the impeller distance from the bottom of vessel, for the ratios of h/d = 1, 2/3 and 1/3 of impeller diameter.

4. Use sliding mesh technique in ANSYS to describe the rotating parts in a jacketed cylindrical agitated vessel mounted with a 45° angle pitched six-blade turbine impeller (PBT).

5. Compare the obtained results with the available literature and propose further improvements to this work.

CHAPTER 2 THEORY OF AGITATED VESSEL

2.1 Introduction

Mixing is a physical operation carried out to reduce non-uniformities in the fluid by eliminating gradients of concentration and temperature. Mixing produces a homogeneity of two different or same components to be perfectly mixed. Mixing can be achieved in chemical industries by mechanical agitation using impeller. This chapter deals with agitated vessels and their types.

2.2 Geometry of agitated vessel

A standardized mechanical stirred agitated vessel is shown in Figure 2.1 and its parts are described below the shape of the base for agitated tanks affects the efficiency of mixing. Depending on application profiles are chosen, like a) flat b) dished c) round d) conical. Industrial applications mostly utilize cylindrical agitated vessel equipped with baffles.
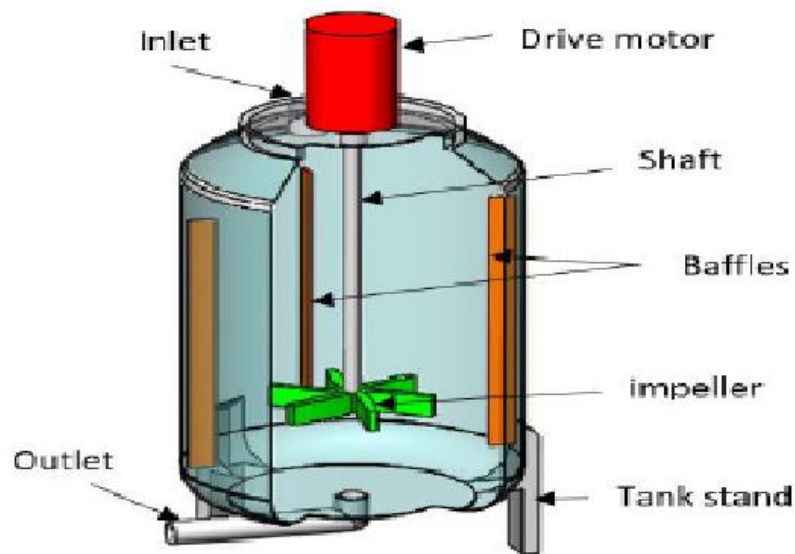
Figure 2.1: Typical configuration of the agitated vessel (Torotwa et al., 2018).

The main components of an agitated vessel are

1. Drive System
2. Shaft
3. Baffles
4. Impeller Types
5. Draft Tubes
6. Inlet and Outlet Ports

Drive system: It constitutes of motor and gearbox of the mixer. The motor can operate by electric DC motor, or driven by air pressure, hydraulic fluid, steam turbine or diesel and gas engine. Standard motor power will be 2984 to 671400 W and above depends on application of mixing agitator. Gearbox is used to obtain the desired mixer shaft speed from the motor speed. A gearbox can have two or three gear reduction and can be fabricated to provide any gear ratio required (Paul et al., 2003).

**Shaft:** Shaft is connected between impeller and drive system. Multiple impellers can be mounted on same the shaft. During the process, liquid vapours or gases should not leak through shaft nozzle and should not exchange external or internal agents of the environment. A most common technique used is sealing shaft with stuffing box.

Baffles: Baffles are vertical strips of metal mounted on walls of the agitated tank, they are installed to eliminate vortexing and swirling and to increase the fluid velocity by diverting the flow across the cylindrical vessel. Generally, the number of baffles used in the agitated vessel are three, four or six. A standard configuration of baffle width b is 1/10 or 1/12 of vessel diameter. Baffles help to change the flow of fluid tangential to vertical flows, provide top to bottom mixing without swirl, and increase the drag and power draw of impeller. Baffles are not used for laminar mixing of viscous fluids (Paul et al., 2003).

Impeller types: A basic classification of fluid flows patterns and impeller types are listed in below table 2.1. Impeller used in transitional and turbulent mixing depending on application shape and geometry are specified in figure 2.2 and 2.3 for six blade pitch blade turbines. For liquid blending and solid suspension, axial flow impeller is suitable for efficient mixing whereas radial flow impellers are best used for gas dispersion. Impeller type and operation conditions are described by Reynolds number and Power number as well as individual characteristics of impeller type. The ratio of impeller diameter is usually 1/3 of vessel diameter. The impeller is placed at h/d = 1/3, 2/3, and 1 distance from the bottom of the agitated vessel, the ratio is chosen on the viscosity of the liquid and liquid level off the bottom.

Axial Flow	Propeller, Pitch Blade Turbine, Hydrofoils
Radial Flow	Flat-Blade impeller, Disk Turbine (Rushton), Hollow-Blade Turbine
High Shear	Cowles, Disk, Bar, Pointed Blade Impeller
Specialty	Retreat Curve Impeller, Sweptback Impeller, Spring Impeller, Glass- Lined Turbine
Up/Down	Disks, Plate, Circles

Table 2.1: Types of impellers and their Flow classification (Paul et al., 2003).
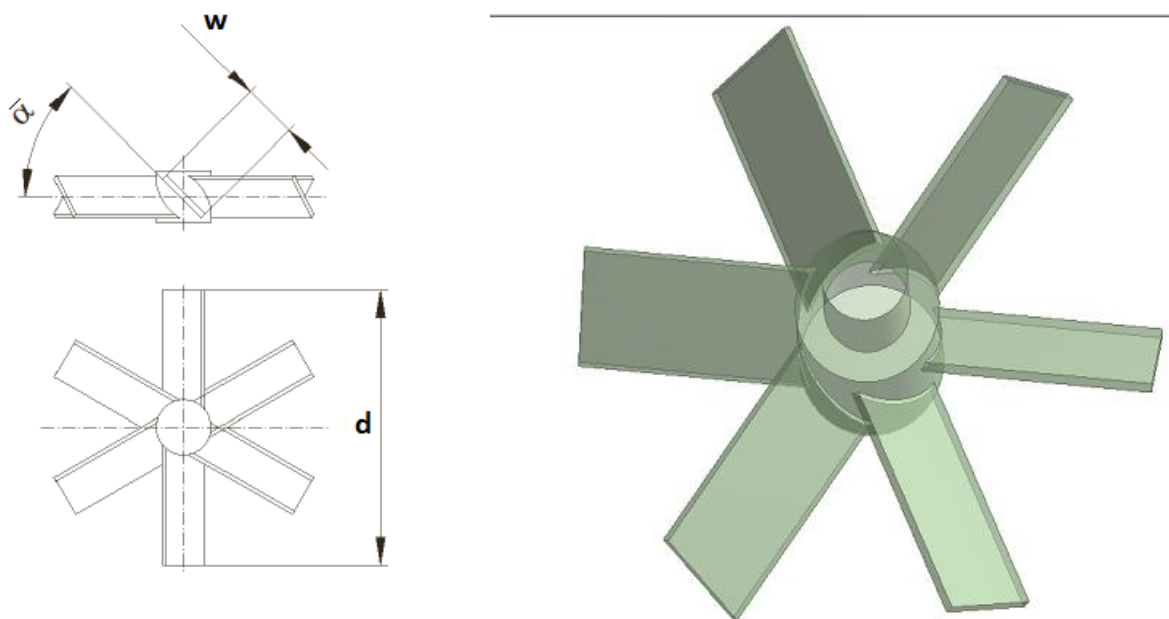
Figure 2.2 - 2.3: Sketch of six blade impellers with $\bar{\alpha} = 45^0$ and design view in ANSYS Design modular. (Beshay et al., 2001).

Draft tubes: A draft tube is cylindrically mounted around impeller and slightly larger in diameter than the impeller. Usually, draft tubes are used with axial impellers to direct suction and discharge streams. An impeller - draft tube system behaves as an axial flow pump with low efficiency. It creates a top to bottom circulation pattern which is important for suspension of solids and for dispersion of gases.

Inlet and Outlet port: The design of inlet and outlets are based on the process and the type of feed and rate of feed dispersion. For the slow batch processes, the inlet can be from the top and quick dispersion rate of the feed, the inlet nozzle should be located at highest location of the vessel where a turbulent region can be formed by inlet flow rate. The outlet

nozzle can be placed at the bottom head of the vessel so that fluid can completely be exuded (Paul et al., 2003).

In standard vessel configuration, the impeller diameter denoted by d, is 1/3 of the vessel diameter D. Impeller height, h, from the bottom of the tank is 1/3 of the vessel diameter. The liquid level is indicated by letter H. The four baffles have a width b of 1/12 of vessels diameter (Brodkey et al., 1998).
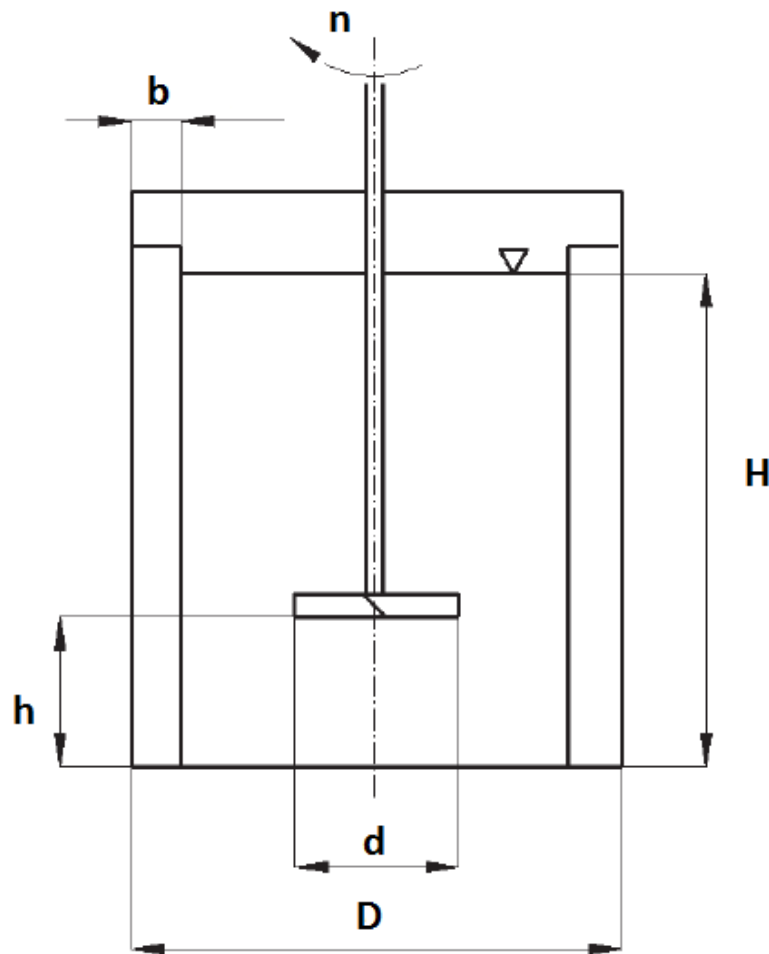
Figure 2.4 Geometric specifications for a stirred tank. (Beshay et al., 2001).

Agitated vessels are useful for liquids of any viscosity up to 750 Pa.s, but although not more than 0.1 Pa.s are rarely encountered through on contacting two liquids for reaction or extraction purposes. In many examples, the contents of agitated vessels are to be heated or cooled and often heating and cooling are required at different portions of liquid level in the production cycle. Heat transfer is an important factor influencing the design of agitated vessels and determine the quality of product outcome. The impeller speed and the agitator selection determine the heat transfer in the system, but other conditions such as the flow

characteristics of the fluid and processing conditions determine the power requirements of the agitator selection primarily in most cases (Chisholm et al., 1988).

The main objectives of agitation in solid-liquid systems can be divided in four categories:

a) To avoid solid accumulation in a stirred tank.

b) Maximize contacting area between solid and liquids.

c) Dispersing a second liquid, immiscible with the first, to form an emulsion or suspension.

d) Raise heat transfer between the liquid and a coil or jacketed vessel. (McCabe et al., 1993).

2.3 Heat transfer surfaces

Heat transfer in an agitated vessel equipped with jackets, an internal helical pipe coil, tube baffles, plate coil baffles and heat exchanger as shown in Figure 2.4.
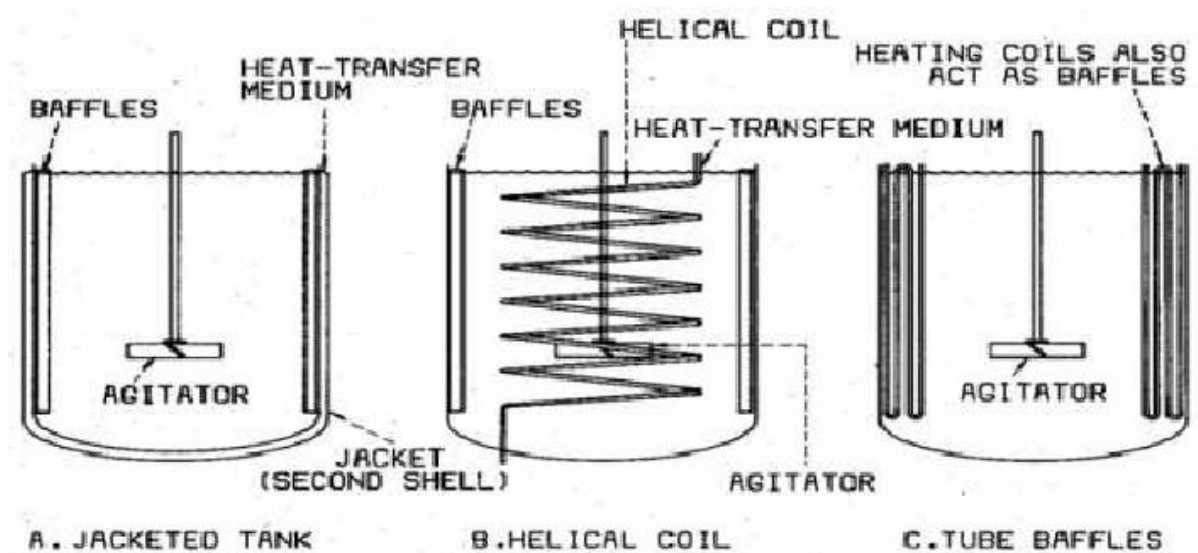
Figure 2.5: Different type of heat transfer equipment for mixing (Singh, 2014).

Selection criteria for most efficient geometry for heat transfer surface are

a) Type of surface.

b) The number of coils, plates, etc.

c) The location of a surface in the vessel.

d) The gap between a coil and banks spacing of harps.

e) Spacing between tubes in harps and helical (Paul et al., 2003).

CHAPTER 3 HEAT TRANSFER IN AGITATED VESSEL

3.1 Heat transfer in agitated vessel

An agitated vessel is used for heating or cooling of agitated fluid. The fundamental heat transfer rate equation can be expressed as

$$Q = \alpha\, S\, \Delta\, \overline{T} \qquad\qquad [3.1]$$

where Q is the heat transfer rate between the agitated liquid and the heat transfer surface, α is heat transfer coefficient, S is the heat transfer area and $\Delta\,\overline{T}$ mean temperature difference (Petera et al., 2010).

3.2 Dimensionless numbers

Dimensionless parameters are needed to calculate heat transfer coefficients and their relations with other parameters in an agitated vessel. Basic dimensionless parameters are explained below.

Reynolds numbers

Reynolds number characterizes the regime of flow i.e. whether the flow is laminar or turbulent. It is a ratio of inertial forces to viscous forces (Petera et al., 2010).

$$\mathrm{Re} = \frac{n\, d^2 \rho}{\mu} \qquad\qquad [3.2]$$

where

n is the rotational speed of the impeller

d is the impeller diameter

ρ is the density of fluid

μ is the dynamic viscosity of the fluid.

Typically, in stirred vessels the Reynolds number varies as follows (Brodkey et al., 1998)

Re < 10 Laminar flow

$10 < \mathrm{Re} < 10^4$ Transitional flow

$\mathrm{Re} > 10^4$ Fully Turbulent flow.

Nusselt number

For calculation of heat transfer in an agitated vessel at the wall or bottom, the Nusselt number is used. Nusselt number is one of important parameters to calculate the heat transfer rate between the fluid and the vessel.

$$\text{Nu} = \frac{\alpha\, D}{\lambda} \qquad\qquad [3.3]$$

where

α is the heat transfer coefficient of the process

D is the diameter of the agitated vessel

λ is the thermal conductivity of the fluid.

Prandtl number

Prandtl number is the ratio between kinematic viscosity and thermal diffusivity. Terms are explained below.

$$\text{Pr} = \frac{v}{a} = \frac{\mu c_P}{\lambda} \qquad\qquad [3.4]$$

μ is the dynamic viscosity of the fluid

c_p is the specific heat capacity

λ is the thermal conductivity of fluid properties.

3.3 Heat transfer correlations for agitated vessel

Agitated vessels in real-time operation where heat addition or removal from the process fluid is required, are equipped with heat transfer surfaces. Mixing operation increases heat transfer intensity in general. A general relation using all dimensionless numbers is usually written as (Petera et al., 2010).

$$\text{Nu} = f\ (\text{Re, Pr, Geometry parameters}) \qquad\qquad [3.5]$$

Correlation for the heat transfer coefficient in an agitated vessel is formed from experiments performed on small scale geometrical similar model of industrial tank

$$\text{Nu} = C\ \text{Re}^a\ \text{Pr}^b\ \text{Vi}^c\ G_d \qquad\qquad [3.6]$$

where

$$\text{Vi} = {\mu_b}/{\mu_w} \qquad\qquad [3.7]$$

Nu is Nusselt number, Re is Reynolds number, Pr is Prandtl number and Vi is the wall viscosity correction factor and G_d is a geometric correction factor. The exponents a, b, c is varied with the parameter constant *C* with the system. Many parameters for the Nusselt number describing the heat transfer in jacketed vessel can be found in Table 3.1 taken from the literature of heat exchanger technology by (Chisholm et al., 1988).

Impeller	N_B(Blades)	Baffles	*C*	Exponents of			Recommended geometric
				Re^a	Pr^b	Vi^c	Corrections G_d
Paddle	2	Yes	0.415	2/3a	1/3	0.24	
		No	0.112	3/4	0.44	0.25	$\left(\frac{Dv}{Di}\right)^{0.40}\left(\frac{L_i}{D_i}\right)^{0.13}$
Various							
Turbines:		No	0.54	2/3	1/3	0.14	$\left(\frac{L_i/Di}{1/5}\right)^{0.15}\left(\frac{N_{bl}}{6}\right)^{0.15}$
Disk, flat 6							$[sin(\theta)]^{0.5}$
Pitched blades		Yes	0.74	2/3	1/3	0.14	$\left(\frac{S_{bl}/D_i}{1/5}\right)^{0.2}\left(\frac{N_{bl}}{6}\right)^{0.2}$
							$[sin(\theta)]^{0.5}$
		No	0.37	2/3	1/3	0.14	$\left(\frac{D_v/Dj}{3}\right)^{0.25}\left(\frac{H_i}{H_i}\right)^{0.15}$
Propeller	3						
		Yes	0.5	2/3	1/3	0.14	$\left(\frac{1.29\,P/D_i}{0.29+P/D_i}\right)$

Table 3.1 Heat Transfer Correlation for Jacketed Vessel with Different Impellers.

a: Relatively low range of Reynolds numbers 20,4000. And other correlations presented in this table were developed for range Re reaching 10^5 and more. For more details, see (Chisholm et al., 1988).

Dittus-Boelter's correlation is generally used in the case of flow in the pipe, in an agitated vessel, it could be used as reference for draft tubes around the impellers (Incropera et al., 2007).

$$Nu = 0.023\, Re^{0.8}\, Pr^{0.33} \tag{3.8}$$

Petera et al. (2017) measured the heat transfer at the bottom of a cylindrical vessel impinged by a swirling flow from impeller in a draft tube using the electro diffusion experimental method by axial flow impeller in the draft tube. A new correlation was proposed from this paper. In equation [3.9] S indicates swirl number (Petera et al., 2017).

$$Nu = 0.041 \, Re^{0.826} \, Pr^{\frac{1}{3}} \, S^{0.609} \qquad [3.9]$$

Petera et al. (2008) performed transient measurement of heat transfer coefficient in an agitated vessel, resulting in the following correlation:

$$Nu = 0.823 \, Re^{\frac{2}{3}} \, Pr^{\frac{1}{3}} \, Vi^{0.14} \qquad [3.10]$$

3.4 Time estimation for heating or cooling of batch of liquid

In industries, agitated vessel is used for batch or continuous reactors. In this case, we are simulating the agitated vessel in batch mode. In practical applications, time of cooling or heating is one of the parameters to operate the batch rector. The mean temperature differences the batch liquid and heating, or cooling depends upon the function of time. The overall heat transfer coefficient U and time for heating or cooling in a batch liquid in an agitated vessel can be estimated by following equations (Chisholm et al., 1988).

The heat transfer rate can be calculated from the equation:

$$Q = m \, c_p \, \frac{dT_b}{dt} = UA(T_h - T_b) \qquad [3.11]$$

where

T_h is the temperature of the heating medium

T_b is the temperature of the batch liquid

m is the mass of batch liquid

c_p is the specific heat capacity of the batch liquid

A is the heat transfer surface area

Equation [3.11] can be rearranged and integrated over the time interval Δt required to heat the agitated liquid from temperature T_{b1} to T_{b2}

$$\int_{Tb1}^{Tb2} \frac{dT}{T_b - T_b} = \frac{U\,A}{W\,C_p} \int_0^{\Delta t} dt \qquad [3.12]$$

which results into:

$$ln\frac{T_h - T_{b1}}{T_h - T_{b1}} = \frac{U\,A}{m\,C_p}\,\Delta t \qquad [3.13]$$

From equation [3.11], the heating time Δt can be calculated, supposing that we know the overall heat transfer coefficient U. This coefficient considers heat transfer coefficients on both sides of the heat transfer surface (Chisholm et al., 1988).

$$\frac{1}{U} = \frac{1}{\alpha_1} + \frac{1}{\alpha_2} \qquad [3.14]$$

CHAPTER 4 POWER CHARACTERISTICS OF IMPELLER

4.1 Power characteristics of impeller

One of the most important parameters in the industrial mixers design of an agitated vessel is power required to drive the impeller and selection of impeller types. For rotation of the impeller inside the agitated vessel, electric motor is required with different torques and power consumptions. One of the factors involved in the cost of equipment is agitated drive system for complex gear boxes because their high speed involves transferring the power input from the driving motor to the impeller frequency of revolution at a moderate level of torque. To determine the power characteristics of the impeller, dimensionless group of Power number needs to be calculated. (Beshay et al., 2001).

4.2 Power Number-Dimensionless group

The power required was calculated from equation [4.1]. The values of torque and angular velocity of the impeller are measured numerically as a monitored quantity in ANSYS Fluent. In experimental setup torque values are measured by using strain gauges etc.

$$P = \tau * \omega \qquad [4.1]$$

τ - Moment (torque)

ω - Angular velocity

Power number is calculated from equation

$$P_o = \frac{P}{\rho * n^3 * d^5} \qquad [4.2]$$

where

P_o is the power number

P is the power

ρ is the density of fluid

n is the rotational speed

d is the diameter of the impeller.

## 4.3 Calculation of power number for 6 blade PBT impeller

In this present work, the input power required for the 6 blade PBT impeller was calculated for the different rotational speeds ranging between 300-900 rpm for the distance of impeller

from the bottom of vessel h/d = 1, 2/3 and 1/3 of impeller diameter (66.66 mm). The results for Power number are tabulated in Table 4.1

| Off-Bottom Clearance	Rotational Speed, n (rpm)	Re [-]	Po [-]
h/d = 1	300	22116	1.62
	500	36860	1.61
	700	51604	1.79
	900	66348	2.01
h/d=2/3	300	22116	1.76
	400	29488	1.66
	500	36860	1.88
	600	44232	1.88
	700	51604	1.88
	800	58976	1.83
	900	66348	1.87
h/d=1/3	300	22116	2.11
	500	36860	2.04
	700	51604	2.00
	900	66348	2.29

Table 4.1: Calculation of Power number.

The graph below represents power characteristics of high-speed impellers operated with baffle vessel, 1 – six-blade turbine with disk(Rushton turbine) (CVS 69 1021),2- six-blade open turbine, 3 – pitched six-blade turbine with pitch angle 45° (CVS 69 1020), 4 – pitched three- blade turbine with pitch angle 45° (CVS 69 1025.3), 5- propeller (CVS 60 1019), 6a,b – high shear stress impeller (CVS 69 10381.2). In this work, we are dealing with pitch blade turbine of pitch angle 45 ° corresponding to the number **3** in Figure 4.1 (Novák et al., 1989).
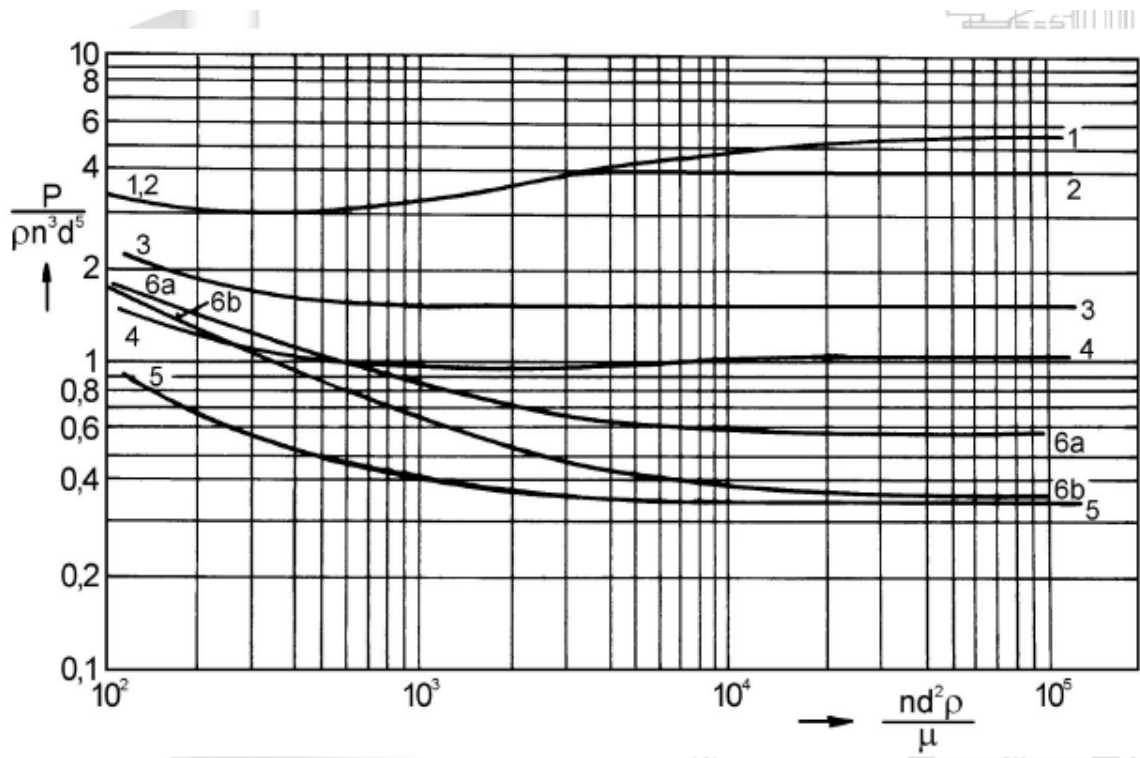
Figure 4.1: Power number vs Reynolds number (log-log scale) (Novák et al., 1989)**.**
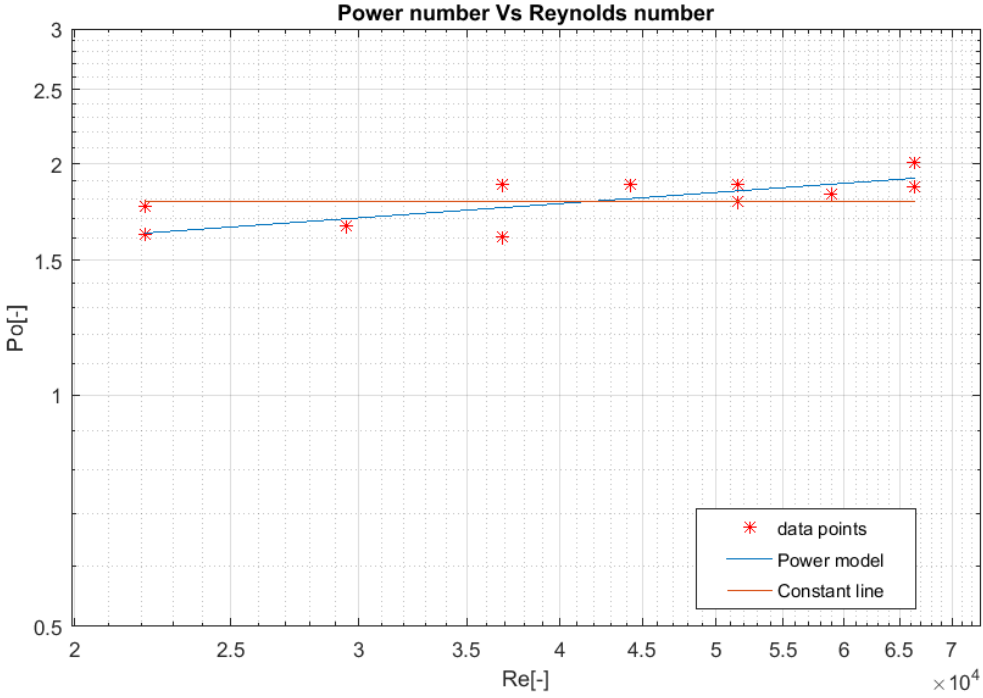
Figure 4.2: Power vs Reynolds number obtained power characteristics of 6 blade PBT impeller, off bottom clearance h/d = 1, 2/3, 1/3. The constant value of Power number based on the null hypothesis was evaluated as 1.78 ± 0.07.

The Power characteristics of PBT impeller can be observed from Figure 4.2. The power model can describe the non-linear relationship between the Reynolds number and Power number as:

$$Po = a \, \mathrm{Re}^b \qquad [4.3]$$

A simpler model can describe the power number as constant only:

$$Po = a \qquad [4.4]$$

where a and b in equation [4.3] are model parameters. The null hypothesis says that the simpler model is good enough compared to the power model from statistical point of view. The power model gives a more accurate description of the functional relationship between the Power number and the Reynolds number. The MATLAB script written for performing non-linear regression function and the 'nlinlfit2' procedure are shown in Appendix E (Chakravarty, 2017). It was found that the power number predicted by the null-hypothesis was 1.78 ± 0.07 (4.30%) which was compared with the average value obtained in experimental work performed by (Beshay et al., 2001). In the calculation of Power number, torsional moment values were taken from ANSYS Fluent solver for corresponding rotational speed of impeller.

4.4 Estimation of mixing time

To express the degree of homogeneity in the agitated vessel containing a batch of liquid to be mixed, an important parameter required is mixing time, t_m. The mixing time depends on different factors such as the size of the tank, impeller size, and type of impeller in an agitated vessel, fluid properties, and impeller rotational speed. The equation used to calculate mixing time expressed as:

$$nt_m = f\left(\frac{n \, d^2 \rho}{\mu}\right) = f(\mathrm{Re}) \qquad [4.5]$$

where nt_m is characterizing the mixing time as dimensionless rotational speed of the impeller, n is the impeller rotational speed in rev/s. For low Reynolds number, the dimensionless rotational speed, nt_m is a function of Reynolds number. In case of higher values of Reynolds number, mixing time nt_m reaches constant value (Novák et al., 1989).

In present work, the rotational speeds of the impeller are ranging 300 to 900 rpm. The simulation run-time was based on the theoretically evaluated mixing time, t_m in agitated vessel. The transient simulations were performed in ANSYS Fluent for seven different

rotational speeds of the impeller 300, 400, 500, 600, 700, 800, 900 rpms and different off bottom clearance h/d = 1, 2/3 and 1/3. The run-time for transient analysis was taken on basis of the mixing time t_m from equation [4.5] for different Reynolds number corresponding to rotational speed. The simulation run time for different rotational speeds is shown in Table 4.2. These times are based on constant value of mixing time $nt_m \approx 50$ (Chakravarty, 2017).

Rotational speed, n (rpm)	Simulation run-time t_m (s)
300	20
400	15
500	10
600	10
700	10
800	10
900	10

Table 4.2: Run-time for simulation.

CHAPTER 5 COMPUTATIONAL FLUID DYNAMICS

5.1 Introduction

The abbreviation CFD stands for computational fluid dynamics. It deals with the area of numerical analysis in the field of fluid's flow phenomena. As sophisticated computer techniques have been developed in recent decades, CFD method is a useful and powerful solving tool for the industrial and non-industrial problems like heat and mass transfer, chemical reaction and predicting fluid flow (laminar, turbulent regime). Some of the applications are:

- Aerodynamic of aircraft and vehicle: lift and drag
- Hydrodynamics of ships
- Power plant: combustion in internal and gas turbine.
- Chemical process engineering: mixing and separation, polymer moulding, external and internal environment of buildings: wind loading and heating/ventilation.
- A lot of other fields where CFD involves: marine, meteorology, biomedical, environment, hydrology, and oceanography engineering.

How does CFD work

CFD contains three main elements:

PRE-PROCESSOR

- ➢ Geometry creation
- ➢ Geometry clean up
- ➢ Mesh generation
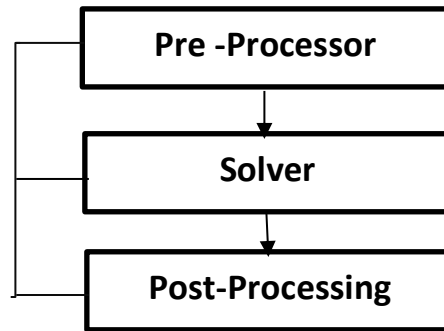- ➢ Boundary conditions

SOLVER

- ➢ Problem specification
- ➢ Additional model
- ➢ Numerical computation

POST – PROCESSING

- ➢ Understanding flow with colour contour etc
- ➢ Vector plots
- ➢ Particle tracking
- ➢ Average values (drag, lift, heat transfer, velocities)

> Report generation

A common CFD solver is mostly based on the finite volume method. Finite element method can be used as well. This means that domain is discretized into finite set of control volumes and general conservation [transport] equations for mass, momentum, energy, species, etc. are solved on this set of control volumes. A finite control volume balance can be expressed as the following where ϕ could be a velocity or enthalpy (Versteeg et al., 2007).

Rate of change of ϕ in the control Volume with respect To time	=	Net rate of increase of ϕ due to convection into the control volume	+	Net rate of increase of ϕ due to diffusion into control volume	+	Net rate of creation of ϕ inside the control volume

5.2 Governing equations of fluid and heat transfer

CFD is based on solving the fundamental governing equations of fluid dynamics - the continuity, momentum, and energy equations which speak about physics. But they are mathematical statements of three fundamental physical principles upon which all of fluid dynamics is depends on

1. Mass is conserved
2. Newton's second law F=ma.
3. Energy is conserved.

These governing equations in conservation form for unsteady, three-dimensional, compressible, viscous flows are discussed in subsequent sections.

5.2.1 Continuity equation

Continuity equation in conservation form is obtained by applying the principle of conversation of mass on a control volume fixed in space and described in differential form is:

$$\frac{\partial \rho}{\partial t} + \nabla \cdot (\rho \vec{u}) = 0 \qquad [5.1]$$

where $\vec{u}$ is the flow velocity at a point on the control volume surface $\vec{u} = f(x, y, z, t)$

and ρ is the density of fluid.

For incompressible flow equation [5.1] simplifies to

$$\nabla . \vec{u} = 0 \qquad [5.2]$$

5.2.2 Momentum equation

Conservation form of momentum equation by the application of Newton's second law of motion to a fixed fluid element is described by three scalar equations X, Y and Z directions for viscous flow called Navier-Stokes equation.

Conservation form is described as:

$$\frac{\partial}{\partial t}(\rho \vec{u}) + \nabla . (\rho \vec{u} \vec{u}) = -\nabla p + \nabla . \vec{\tau} + \rho \vec{f} \qquad [5.3]$$

where $\nabla \cdot \vec{\tau}$ is the viscous tensor and $\vec{f}$ is body force per unit mass.

Navier-Stokes equation in terms of X, Y and Z components as:

X- component of momentum equation:

$$\frac{\partial(\rho u_x)}{\partial t} + \nabla \cdot (\rho u_x \vec{u}) = -\frac{\partial p}{\partial x} + \frac{\partial \tau_{xx}}{\partial x} + \frac{\partial \tau_{yx}}{\partial y} + \frac{\partial \tau_{zx}}{\partial z} + \rho f_x \qquad [5.4]$$

Y-component of momentum equation:

$$\frac{\partial(\rho u_y)}{\partial t} + \nabla \cdot (\rho u_y \vec{u}) = -\frac{\partial p}{\partial y} + \frac{\partial \tau_{xy}}{\partial x} + \frac{\partial \tau_{yy}}{\partial y} + \frac{\partial \tau_{zy}}{\partial z} + \rho f_y \qquad [5.5]$$

Z-component of momentum equation:

$$\frac{\partial(\rho u_z)}{\partial t} + \nabla \cdot (\rho u_z \vec{u}) = -\frac{\partial p}{\partial z} + \frac{\partial \tau_{xz}}{\partial x} + \frac{\partial \tau_{yz}}{\partial y} + \frac{\partial \tau_{zz}}{\partial z} + \rho f_z \qquad [5.6]$$

5.2.3 Fourier-Kirchhoff equation (Energy equation)

The primary aim of the energy transport equations is the calculation of temperature field given velocity's, pressures, and boundary conditions. Temperatures can be derived from the calculated enthalpy (or internal energy) using thermodynamics relationship

$$\frac{Dh}{Dt} = C_P \frac{DT}{Dt} + \left(v - T\left(\frac{\partial v}{\partial T}\right)_p\right)\frac{DP}{Dt} \qquad [5.7]$$

Giving the transport equation for temperature

$$\rho c_P \left[\frac{\partial T}{\partial t} + \vec{u} \cdot \nabla T\right] = \lambda \nabla^2 T + \vec{\vec{\tau}} : \vec{\vec{\Delta}} + \dot{q}^{(g)} \qquad [5.8]$$

Where C_p is specific heat at constant pressure, T is absolute temperature, $\vec{\vec{\tau}}$ is dynamic stress tensor, $\vec{\vec{\Delta}}$ is symmetric part of the velocity gradient tensor and $\dot{q}^{(g)}$ is internal heat sources or sink (it is necessary to include also reaction, phase changes, enthalpies and electric heat).

5.3 Turbulence

In real world, most of engineering problem is related to turbulence. It is very difficult to give a precise definition of turbulence. Some of the characteristics of turbulent flow: (ANSYS Fluent 13.0 Training material, 2010).

- Enhanced Diffusivity
- Enhanced dissipation
- Large Reynolds number
- Three-Dimensionality
- Vorticity fluctuation
- Fractalization Mechanisms

Overview of computational approaches

There are three basic approaches that can be used to calculate a turbulent flow:

Direct Numerical Simulation (DNS)

- It is technically possible to resolve every fluctuating motion inflow.

- The meshing of the grid should be very fine and number of timestep very small.

- Demands increase with Reynolds number.

- DNS is only a research tool for lower Reynolds number flow.

- Restricted to supercomputer applications.

Large Eddy Simulation (LES)

- In terms of computational demand, LES lies in between DNS and RANS.

- Like DNS, a 3D simulation is performed over many timesteps.

- Only the large 'eddies' are resolved.

- The grid can be coarser and timesteps larger than DNS because the smaller fluid motion is represented by a sub-grid-scale (SGS) model.

Reynolds Averaged Naiver Stokes Simulation (RANS)

- Many different models are available.

- Still the most frequently used approach.

- Equations are solved for time-averaged flow behaviour and the magnitude of turbulent fluctuations.

- All turbulent motion is modelled.

5.3.1 RANS Turbulence modelling

A turbulence model is defined as a set of algebraic or differential equations which determine the turbulence transport terms in the mean flow equations and close to the system of equations. In fluids, the turbulent flow is characterized by random fluctuations of transport quantities such as flow velocity, pressure, temperature, etc.
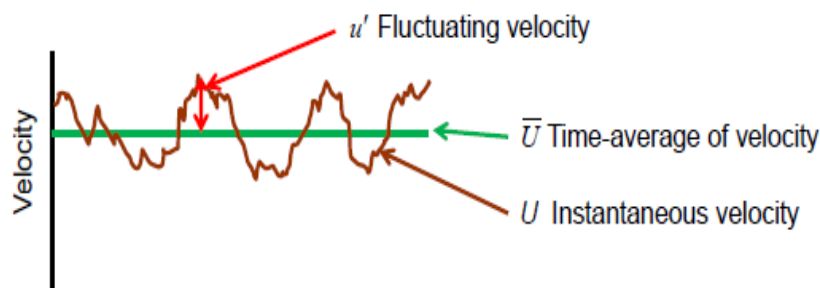
Figure 5.1: Instant velocity in a turbulent flow. (ANSYS 13.0 Training material, 2010).

At any point in time, the actual velocity can be decomposed to the mean velocity and fluctuating velocity component:

$$U = \bar{U} + u'$$ [5.9]

where

U is the actual velocity

$\bar{U}$ is the time average of velocity (mean velocity)

u' is the fluctuating velocity component.

In Navier-Stokes equation which governs the velocity and pressure of the fluid flow, the time-dependent velocity fluctuations are separated from the mean flow velocity by the averaging of the Navier-Stokes equation and the resulting equation obtained is called Reynolds averaged Naiver-Stokes (RANS) equation can be written as:

$$\frac{\partial \rho}{\partial t} + \frac{\partial (\rho \pi_i)}{\partial x_i} = 0$$ [5.10]

$$\frac{\partial (\rho \bar{u}_i)}{\partial t} + \frac{\partial (\rho \bar{u}_i \bar{u}_i)}{\partial x_j} = -\frac{\partial \bar{P}}{\partial x_i} t \frac{\partial}{\partial x_j} \left[u \left(\frac{\partial \bar{u}_i}{\partial x_j} + \frac{\partial \bar{u}_j}{\partial x_j} - \frac{2}{3} \delta_{ij} \frac{\partial \bar{u}m}{\partial x_m} \right) \right] + \frac{\partial}{\partial x_j} - \rho \overline{\bar{u}_i u'_j}$$ [5.11]

where

$\rho \bar{u}_i \bar{u}_j$ is a Reynolds stress tensor, R_{ij}

RANS model falls into one of two categories. The difference in these is how the Reynolds stress term $\bar{u}_i \bar{u}_j$ in the previous equation [5.11] is modelled. By introducing the concept of eddy turbulent viscosity (EVM), the following equation can be used:

$$-\rho \bar{u}_i \cdot \bar{u}_j = \mu_t \left(\frac{\partial \bar{u}_i}{\partial x_j} + \frac{\partial \bar{u}_j}{\partial x_i} \right) - \frac{2}{3} \delta_{ij} \left(\rho_k + \mu_t \frac{\partial \bar{u}_m}{\partial x_m} \right)$$ [5.12]

where

μ_t is the turbulent viscosity

$$\mu_t = \rho c_\mu \frac{k^2}{\varepsilon}$$ [5.13]

In equation [5.13], k represents the turbulent kinetic energy, ε represents kinetic energy dissipation rate and c_μ is empirical constant. Quantities k and ε then described by other transport equations (ANSYS 13.0 Training material, 2010).

5.3.2 Turbulence models available in Fluent

One-Equation model
Spalart-Allmaras
Two-Equation Models
Standard k-ε
RNG k-ε
Realizable k-ε
Standard k-ω
SST k-ω
Reynolds Stress Model
k-kl-ω Transition Model
SST Transition Model

Table 5.1: Turbulence Model in ANSYS Fluent (ANSYS Training material, 2014).

5.4 k-ω SST Turbulence model

In present work, k-ω Shear-Stress-Transport (SST) turbulence model is chosen to perform simulation in an agitated vessel. It is hybrid of two model in which k-ω model is used near the wall and k-ε model in the free stream. k represents the turbulent kinetic energy ε which is explained in equation [5.13] and ω is specific dissipation rate. k-ω is most widely adopted in the aerospace, turbo-machinery, and heat transfer applications (ANSYS Training material, 2014).
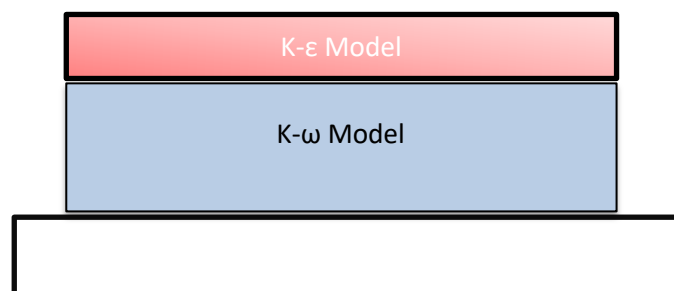
Figure 5.2: k-ω SST Turbulence model blends with k-ω & k-ε.

The transcription equations for k-ω SST model are (ANSYS Fluent 6.1 User's Guide,2003):

$$\frac{\partial}{\partial t}(\rho k) + \frac{\partial}{\partial x_i}(\rho k u_i) = \frac{\partial}{\partial x_j} = \left(\Gamma_k \frac{\partial k}{\partial x_j}\right) + \tilde{G}_k - Y_k + S_k \qquad [5.14]$$

$$\frac{\partial}{\partial t}(\rho \omega) + \frac{\partial}{\partial x_i}(\rho_\omega u_i) = \frac{\partial}{\partial x_j}\left(\Gamma_w \frac{\partial \omega}{\partial x_j}\right) + G_\omega - y_\omega + D_\omega + S_\omega \qquad [5.15]$$

In these equations [5.14] and [5.15] the terms $\tilde{G}_k$ represents the generation of turbulent kinetic energy which is same as in standard k-ω model. G_ω represents the generation of ω, Γ_k and Γ_ω represent effective diffusivity of k and ω. Y_k and Y_ω represents dissipation of k and ω due to turbulence, $D\omega$ represents cross-diffusion, s_k and s_ω are the user-defined source terms (ANSYS Fluent 6.1 User's Guide, 2003).

5.4.1 Turbulent boundary layers

A turbulent boundary layer consists of distinct regions. For CFD, the most important is the viscous sublayer, immediately adjacent to the wall, and slightly further away from the wall is the log layer.
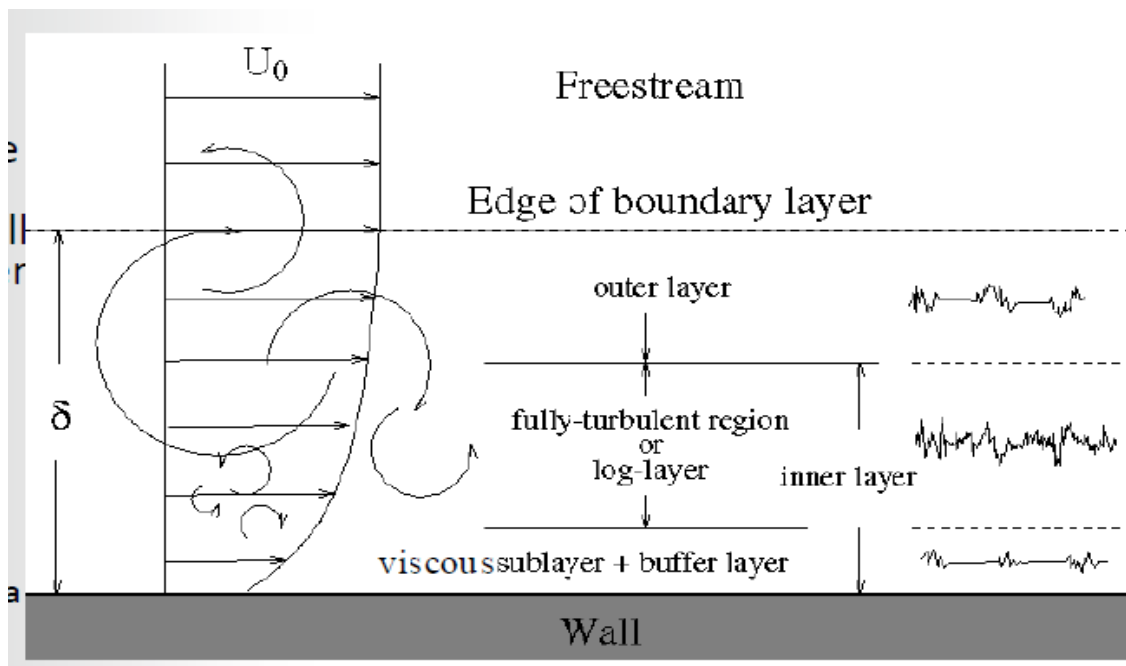
Figure 5.3: Describing turbulence boundary layers (ANSYS 15.0 Training material, 2014).

Near to a wall, the velocity changes rapidly. The velocity is made dimensionless, defined as:

$$u^+ = \frac{u}{u_\tau}; u_\tau = \sqrt{\frac{\tau_{wall}}{\rho}} \qquad\qquad [5.16]$$

where

u is the velocity of the flow

τ_{wall} is the wall shear stress

ρ is the density of fluid

The distance is made dimensionless:

$$Y^+ = \frac{Y u_\tau}{\nu} \qquad\qquad [5.17]$$

Where Y is the distance from the wall, which represents the dimensionless boundary layer profiles. The size of your grid cell nearest to the wall value of Y^+ is very important. In the near-wall region, the solution gradients are very high, accurate calculations in the near-wall region are necessary for the best solution of numerical simulations. First grid cell needs to be at about $Y^+ = 1$ and a prism layer mesh with growth rate no higher than = 1.2 is recommended. This is an approach you will take and is recommended for turbulence model SST k-ω. Using a wall fall function the first grid cell size should be with in range to be 30 < Y^+ < 300 (ANSYS 15.0 Training material, 2014).
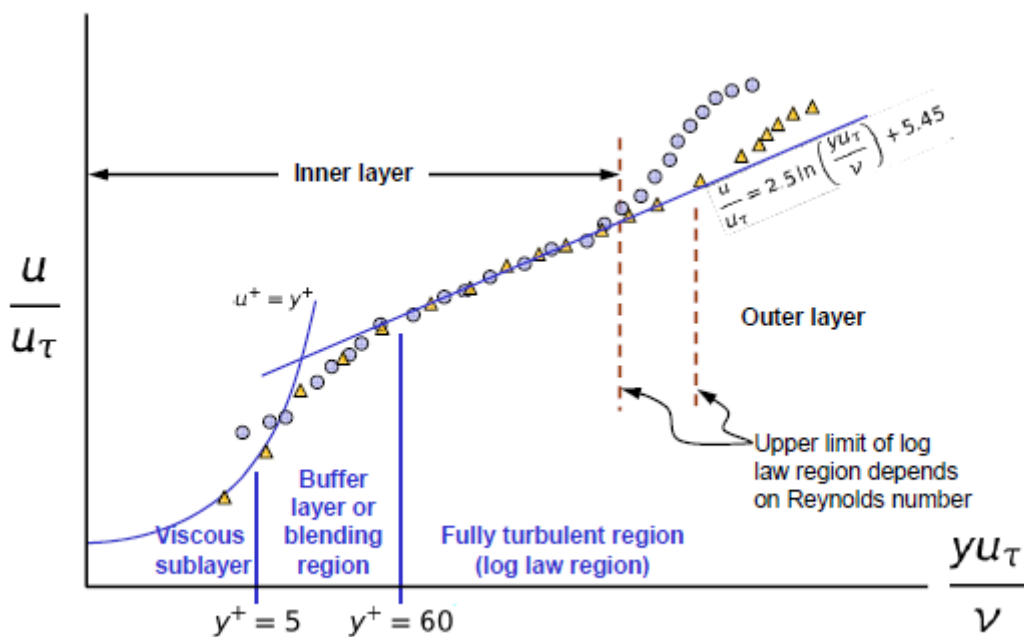
Figure 5.4: The universal law of wall model (ANSYS 15.0 Training materials, 2014).

5.5 Meshing

Meshing is a pre-processing step for the computational fluid simulation. The whole geometry domain space of interest is discretised into small cells known as 'the grid', or mesh. ANSYS CFD uses Finite Volume Methods (FVM). The grid can be of many shapes and sizes. For example, the elements are either quadrilaterals, triangles, tetrahedral, prisms, pyramids or hexahedra. These shapes are for 2D and 3D geometry. See the next figure for illustrations of some element types.
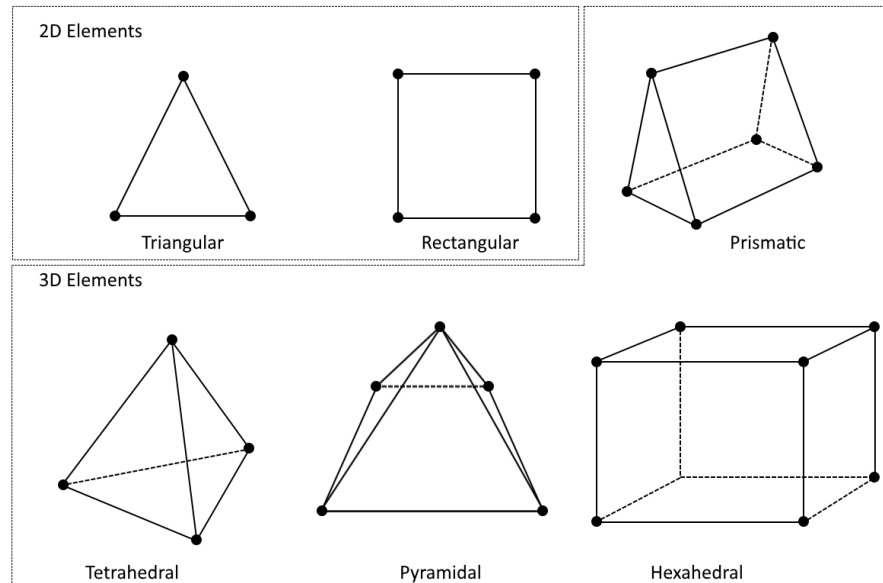
Figure 5.5: Mesh element types used in computational grids (Edward et al., 2003).

5.5.3 Mesh quality metrics

A good mesh is required for best solutions to minimize the error in Fluent solver. Good mesh has three components which are good resolution, appropriate distribution, and good mesh quality. To decide the mesh quality, ANSYS provides several mesh metrics, most important are:

1. Orthogonal Quality (OQ)

2. Skewness

The low orthogonal quality or high skewness values are not recommended. Generally, try to keep minimum orthogonal quality >0.1, or maximum skewness <0.95, these values may be different on the physics and location of the cell. ANSYS Fluent solver can display the mesh orthogonal quality only. (ANSYS 15.0 Training material, 2014).

Skewness mesh metrics spectrum					
Excellent	Very good	Good	Acceptable	Bad	Unacceptable
0-0.25	0.25-0.50	0.50-0.80	0.80-0.94	0.95-0.97	0.98-1.00

Orthogonal Quality mesh metrics spectrum					
Unacceptable	Bad	Acceptable	Good	Very good	Excellent
0-0.001	0.001-0.14	0.15-0.20	0.20-0.69	0.70-0.95	0.95-1.00
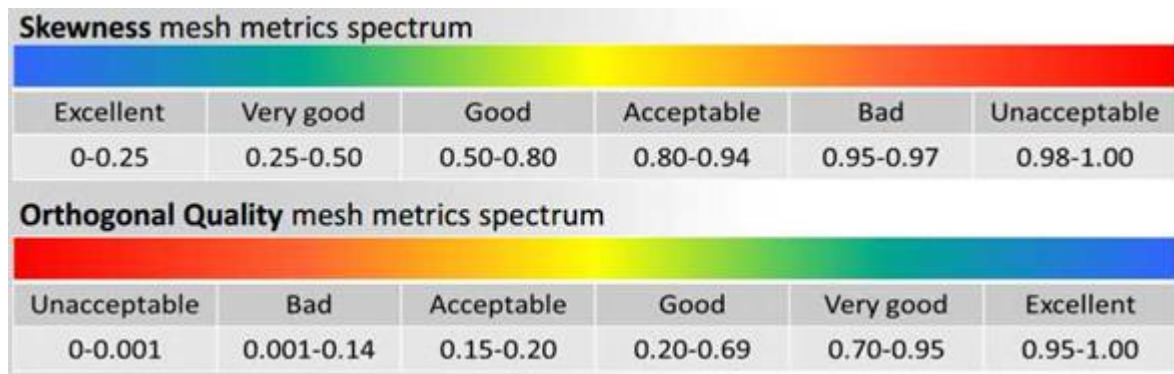
Figure 5.6: Skewness and Orthogonal mesh quality (ANSYS 15.0 Training material, 2014).

5.6 Modelling the flow around impeller

ANSYS Fluent tool provides the solution for rotating parts in a fluid like impeller, rotating blades and moving walls. To consider the effect of rotating parts in geometry, there are two different techniques available in ANSYS Fluent. They are

1) Moving reference frame (MRF)
2) Sliding mesh technique

5.6.1 Sliding mesh technique

In the present work, simulation is carried out by using sliding mesh technique. The fluid zone around the impeller rotates inside the baffled agitated vessel. Therefore, to take account of baffles and their interaction with the rotating impeller, sliding mesh technique must be used in a time-dependent solution in which grid surrounding the rotation components moves during each time step. The motion of impeller is realistically modelled with this approach, giving rise to a time-accurate simulation of impeller-baffle interaction. The sliding mesh technique is the most rigorous and informative solution method for agitating vessel simulations. Transient simulations using this model can capture low-frequency oscillations in the flow field. The sliding mesh technique is similar to the MRF model when modeling a separate fluid region for the impeller and the vessel. But, with sliding mesh, the impeller region is disconnected from mesh of the agitated vessel by using the in ANSYS Design modeler tool and ANSYS Meshing. In the tank region the standard conservation equations for mass and momentum are solved. In the rotating impeller region, modified set of balance equations is solved. [5.18] represents the modified continuity equation and [5.19] is modified momentum balance: (Bakker et al., 1997).

$$\frac{\partial}{\partial x_j}(u_j - v_j) = 0 \qquad [5.18]$$

$$\frac{\partial}{\partial t}\rho u_i + \frac{\partial}{\partial x_j}\rho(u_j - v_j)u_i = \frac{-\partial p}{\partial x_i} + \frac{\partial \tau_{ij}}{\partial x_j} \qquad [5.19]$$
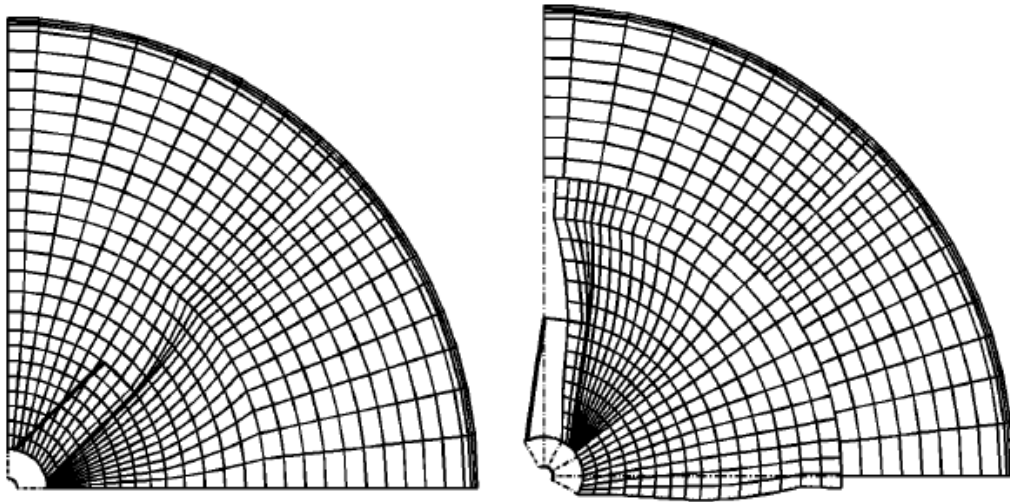
where

u_j is the liquid velocity in stationary reference frame.

v_j is the velocity component arising from mesh motion.

p is the pressure.

τ_{ij} is the stress tensor.

Figure 5.7: Illustration of grid motion in the sliding mesh method at two different time steps. Mesh is moving with impeller region and slides with the stationary region for the rest of agitated vessel (Bakker et al., 1997).

CHAPTER 6 NUMERICAL METHODOLOGY AND MODEL DESCRIPTION

6.1 Introduction

This chapter presents description of the problem statement, geometrical configurations, meshing, Y^+ values and grid convergence index.

6.2 Problem statement

In present work, CFD simulations of heat transfer in a baffled agitated vessel by pitched blade turbine (PBT) with six blades and pitched angle 45° were preformed Constant heat flux $q = 3000 \, W/m^2$ was applied to the bottom and vertical walls of the vessel. Heat transfer coefficients were evaluated at the bottom and vertical walls for different rotation speeds (300 to 900 rpm) and different impeller distances from the bottom of vessel (ratios of h/d = 1/3, 2/3, 1).
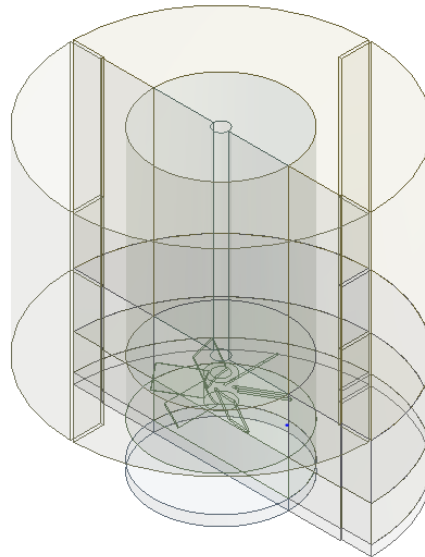
Figure 6.1: Agitated vessel designed in ANSYS Design Modeler.

6.3 Geometrical configuration

The system under investigation is the flat-bottom, baffled cylindrical agitated vessel equipped with six-blade 45° Pitched blade turbine (PBT). The agitated vessel is filled with water up to the level D=H. Designed model of agitated vessel is shown in Figure 6.1. Water was chosen as the liquid medium in this primary study. Default water properties were chosen in ANSYS Fluent database for simulations. The dimensions of the agitated vessel, impeller and fluid properties are shown in tables 6.1 and 6.2.

Item	Symbol	Dimension
Vessel diameter	D	0.2 m
Vessel height/liquid height	H	0.2 m
Impeller diameter	d = D/3	0.0666667 m
Width of impeller blade	w	0.02 m
off-bottom clearance	$h = d\ (1\ ,\frac{2}{3},\frac{1}{3})$	0.066667, 0.04444, 0.02222 m
Blade thickness	t	0.001 m
No. of Blades	n_B	6
Pitch angle	$\bar{\alpha}$	45°
Baffle width	b	0.02 m
Number of baffles	B	4
Baffle thickness	b_t	0.002 m

Table 6.1: Agitated vessel dimensions

Item	Symbol	Value
Density	ρ	998.2 Kg / m^3
Dynamic viscosity	μ	0.001003 Pa. s
Specific heat	Cp	4182 J/Kg K
Thermal conductivity	λ	0.6 W/m K

Table 6.2: Fluid properties ANSYS Fluent values.
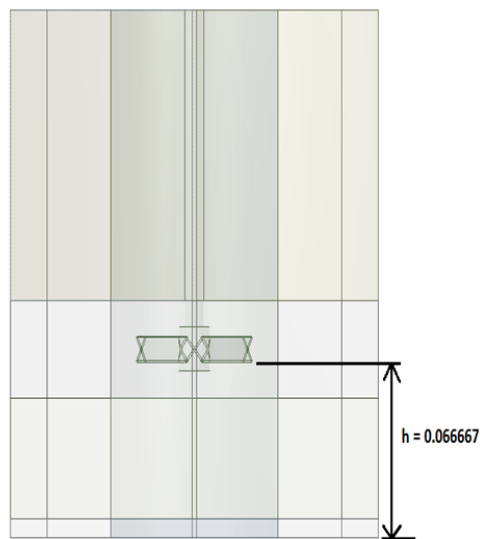
Figure 6.2: Agitated vessels off-bottom clearance with 1, 2/3, 1/3 h = 0.066667 m, h = 0.04444, h= 0.02222m.

6.4 Computational grid

The modelled geometry was discretized using hexahedral and tetrahedral elements in ANSYS meshing for off-bottom clearance h/d = 1, 2/3, 1/3 of an agitated vessel. Tetrahedral mesh was generated around the impeller region and rest of domain was discretized by hexahedral elements. The total number of mesh elements generated was around 2.2 million. The computational grid generated in ANSYS Meshing is shown in Figure 6.3, Figure 6.4 and Figure 6.5.
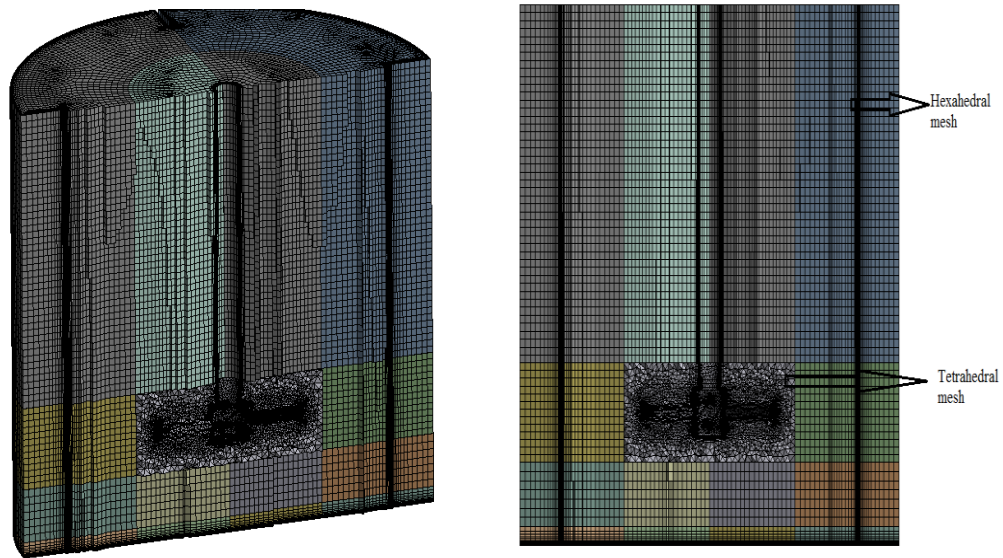
Figure 6.3 - 6.4: Computational grid of agitated veseel (isometric view and xy plane).
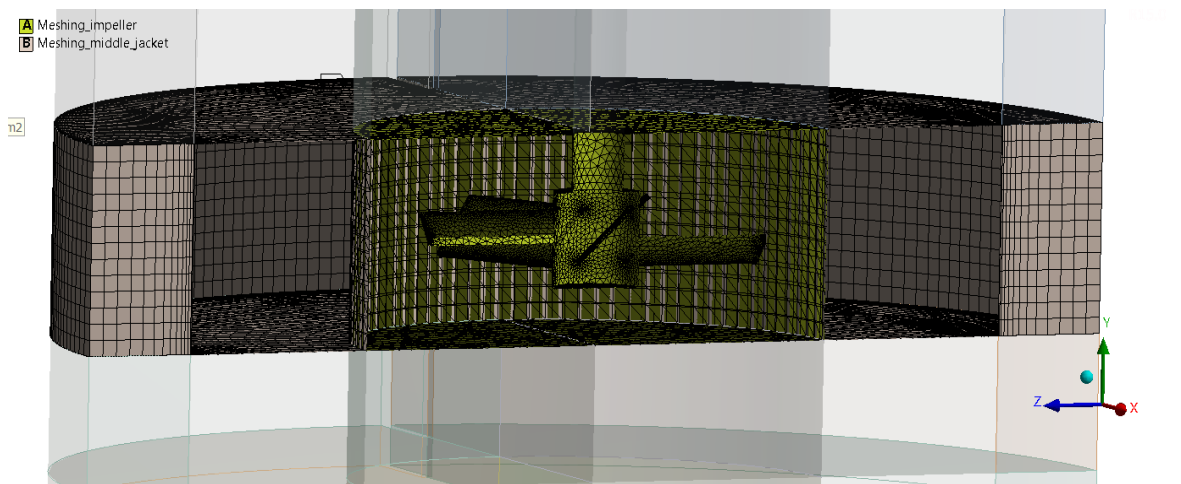
Figure 6.5: Tetrahedral mesh elements around impeller region.

6.5 Mesh quality

As it was discussed in chapter 5 (Figure 5.6) about mesh quality, parameters like skewness, orthogonal quality, aspect ratio, etc can be used. The values obtained for the mesh of 2.2 million elements of computational grid of agitated vessel are tabulated in Table 6.3.

Quality Measure	Value
Maximum Skewness	0.97
Minimum Orthogonal Quality	0.0372163
Maximum Aspect Ratio	4.14472e+02

Table 6.3: Mesh quality measures for h/d= 2/3, 500rpm.

Accuracy of the simulation results depends upon the quality of the generated mesh of the geometry. The obtained values of mesh quality (skewness, orthogonal, aspect ratio) were not satisfying. In ANSYS Fluent, there is option to convert the tetrahedral mesh elements into polyhedral mesh. After the polyhedral conversion, the quality of mesh improved substantially, and total number of elements decreased to 1.7 million. Polyhedral meshing gives better accuracy results and faster runtime solutions. Maximum skewness 0.80-0.93 is acceptable, 0.89 lies in between.

Quality Measure	Value
Maximum Skewness	0.89
Minimum Orthogonal Quality	0.105521
Maximum Aspect Ratio	4.14472e+02

Table 6.4: Mesh quality measures for generated grid for h/d= 2/3, 500rpm after conversion of tetrahedral to polyhedral mesh elements.
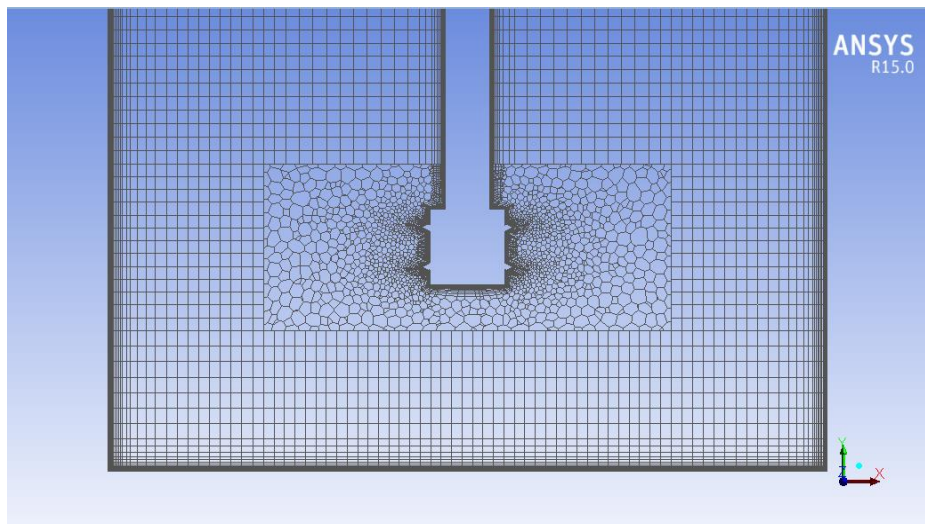
Figure 6.6: Polyhedral mesh elements around impeller region.

The mesh quality measures were then assumed to be satisfactory for further steps in ANSYS Fluent simulations.

6.6 Checking Y^+ value at the tank walls

Y^+ values are important when it comes to accurate description of gradients near walls as it was mentioned in previous chapter. First grid cell needs to be at about $Y^+=1$ so that no wall functions must be used to approximate gradients near walls. In our case number of inflation layer near the bottom and walls of agitated vessel is around 17 layers. After performing the simulations, values of Y^+ were checked for the bottom and walls of vessel for the 900 rpm. See the following figure
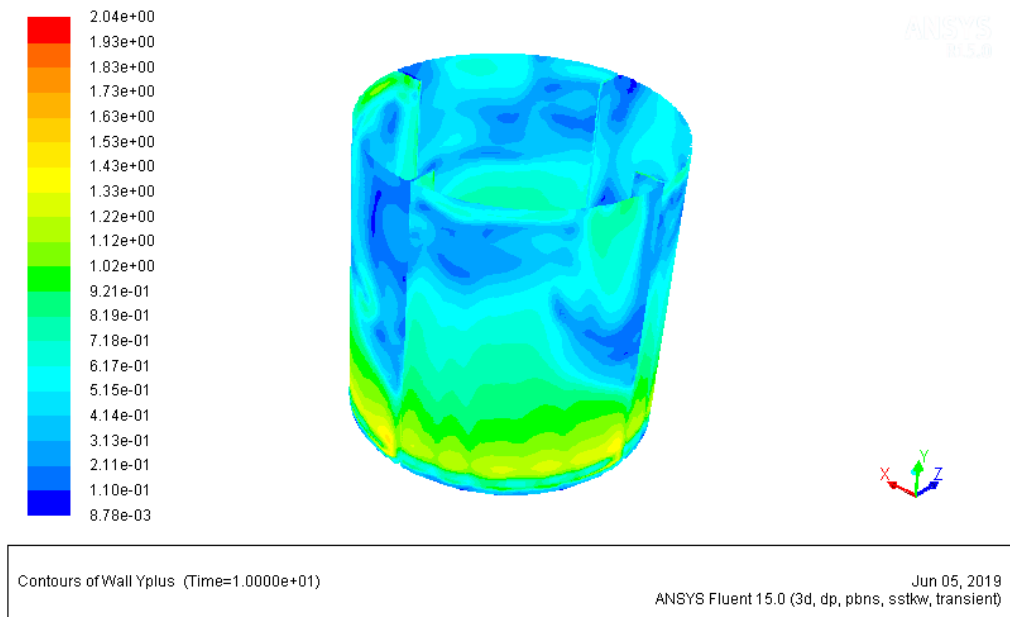
Figure 6.7: Y^+ range for bottom and walls of vessel 900 rpm, h/d =2/3.

6.7 Grid Convergence Index (GCI)

The examination of the spatial convergence of a simulation is direct method for determining the ordered discretization error, in other words, the accuracy of a CFD simulation. This method involves performing the simulations on two or more finer grids. As the grid is refined, the number of cells in the flow domain increases. The spatial and temporal discretization error should asymptotically come to zero, excluding computer round off-error (Celik et al., 2008).

The dependency of solution on the number of mesh (grid) cells (elements) can be described by the following equation

$$\Phi = \Phi_{\text{ext}} + aN^{-p/D} \qquad [6.1]$$

N represents the number of mesh elements, D is equal to 2 in 2-D case or 3 in 3-D case. The number of mesh elements powered to -1/D represents a value which is proportional to mesh element size, for example, it should be 0.1 for two-dimensional mesh 10x10 and 0.01 for mesh 100x100. We have three unknow parameters in the equation above, Φ_{ext} , a and p. Parameter p represents here the order of the solution accuracy, the larger is its value the better, Φ_{ext} represents the extrapolated value of the solution for the infinitely large number of mesh elements. There values from solution of 3 equation can written for 3 different mesh sizes.

$$\Phi_1 - \Phi_{ext} - aN_1^{p/D} = 0 \qquad\qquad [6.2]$$

$$\Phi_2 - \Phi_{ext} - aN_2^{p/D} = 0 \qquad\qquad [6.3]$$

$$\Phi_3 - \Phi_{ext} - aN_3^{p/D} = 0 \qquad\qquad [6.4]$$

After solving these equations, according to (Celik et al., 2008), the parameter p can be calculated as follows

$$p = \frac{1}{ln\, r_{21}} \left|ln \left|\frac{\varepsilon_{32}}{\varepsilon_{21}}\right| + ln \left(\frac{r_{21}^P - s}{r_{32}^P - s}\right)\right. \qquad\qquad [6.5]$$

where

$$\varepsilon_{32} = \Phi_3 - \Phi_2\ ,\ \ \varepsilon_{21} = \Phi_2 - \Phi_1$$

$$r_{21} = \frac{N_2}{N_1}\ ,\ r_{32} = \frac{N_3}{N_2}$$

$$s = sign\, \frac{\varepsilon_{32}}{\varepsilon_{21}}$$

The absolute values and the sign function are considered in cases of non-monotonous increase or decrease of the monitored quantity. For example ($\Phi_1 < \Phi_2$) and ($\Phi_2 > \Phi_3$). To obtain the value of parameter p, equation [6.5] solved numerically

Then the extrapolated value of the monitored quantity can be expressed as:

$$\Phi_{ext} = \frac{\Phi_1 r_{21}^p - \Phi_2}{r_{21}^p - 1} \qquad\qquad [6.6]$$

The accuracy of the solution for each value of Φ is expressed as the difference between the measured value and the extrapolated value and can be expressed in terms of the grid

convergence index (GCI). The smaller value GCI is the more accurate is the measured value. The following equation can calculate GCI.

$$GCI_{21} = F_S \frac{\Phi_{exp} - \Phi_1}{\Phi_1} \qquad [6.7]$$

Substituting for Φ_{exp} could give

$$GCI_{21} = \frac{1.25e_a^{21}}{r_{21}^p - 1} \qquad [6.8]$$

where 1.25 represents safety F_s in the estimation of numerical accuracy, and e_a^{21} is defined as equation [6.9] and r_{21} represents the ratio of elements sizes.

$$e_a^{21} = \left| \frac{\Phi_1 - \Phi_2}{\Phi_1} \right| \qquad [6.9]$$

Similar definition could be derived for the mid-size mesh

$$GCI_{32} = \frac{1.25e_a^{32}}{r_{32}^p - 1} \qquad [6.10]$$

It is recommended that the refinement ratios r_{21}^p and r_{32}^p be greater than value 1.3 (Celik et al., 2008).

6.8 Calculation of Grid Convergence Index

The GCI values for the same geometry were already evaluated by Chakravarty, (2017). He discretized the geometry of the agitated vessel into three different mesh sizes of 1080381, 2269507 and 4564764 elements. Chakravarty (2017) performed simulations in ANSYS Fluent for a rotational speed of 500 rpm with moving reference frame (MRF) technique modeling flow around the impeller. Calculated average values of torque τ were used to evaluate the GCI_{21} and GCI_{32} for the finer mesh and mid-size mesh. By using 'fsolve' procedure in MATLAB, parameter p can be determined numerically. Chakravarty found the values of fine-grid (4564764) solution was 0.88% and for the mid-size grid (2269507) solution 1.08%. The calculated GCI values with numerical accuracy parameters are tabulated in Table 6.5. In present work number of mesh elements generated in ANSYS Meshing was 2167821 which is similar to the mid-size mesh by Chakravarty. Its accuracy was reported as 1.08% which seemed to be sufficient and this mesh was then used in all simulations in this

thesis (conversion of tetrahedral to polyhedral mesh elements was used to improve the mesh quality).

	$\Phi = M_t$ at 500 rpm (non-monotonic dependency)
N_1, N_2, N_3	4564764, 2269507, 1080381
r_{21}	1.26
r_{32}	1.28
Φ_1	2.4587476737e-02
Φ_2	2.4640680896e-02
Φ_3	2.4570484468e-02
p	1.1492
Φ_{ext}^{21}	0.0244
e_a^{21}	0.21 %
GCI_{fine}^{21}	0.88 %
e_a^{32}	0.28 %
$GCI_{mid-size}^{32}$	1.08 %

Table 6.5: Calculation of discretization error (Chakravarty, 2017).

CHAPTER 7 CFD SIMULATION OF HEAT TRANSFER IN AGITATED VESSEL

7.1 Introduction

The section in this chapter explains the set-up of ANSYS Fluent 15.0 and boundary conditions to obtain the heat transfer coefficients in a baffled agitated vessel with a six blade PBT impeller and study the effect of heat transfer at bottom and vertical walls for different rotational speeds and off-bottom clearances from the impeller.

7.2 Solution procedure

ANSYS Fluent software was used to perform the CFD simulation of discretized model of agitated vessel. As the number of mesh elements generated was more than 2 million (2167821), simulations were performed at the faculty computational servers (256 GB RAM) provided by Czech Technical University. To save the simulation time, parallel simulation was performed in personal computer with I5 Processer with 12 GB RAM. At the university servers, run time of 10 seconds took 7-9 days, and at personal computer more than 30 days for simulated time.

ANSYS Fluent journal file including all the commands for execution by the solver of ANSYS Fluent in batch mode were created for different rotational speeds and run times with heat flux q = 3000 W/m^2.

Example of journal file written for rotational speed of 300 rpm and simulation run time 20 seconds (refer Table 5.2 for different rpms and runtime) is shown below:

```
; fluent150t 3ddp -t 16 -g -i fluent.in
/file/read-case-data init-hs.cas.gz
;
; will overwrite files without a confirmation
/file/confirm-overwrite no
;
/mesh/reorder/reorder-domain
;
; rotation speed definition
/define/parameters/input-parameters edit "rotation-speed" "rotation-speed" 300
;
; first - switch energy off and perform some steady-state iterations
/define/models energy no
```

```
/define/models steady yes
/solve/iterate 2000
; save steady-state
/file/write-case-data steady.cas.gz
;
; switch to transient model
/define/models unsteady-1st-order yes
; switch energy on + dissipation: no, pressure work: no, kinetic energy: no,
;   diffusion at inlets: yes
/define/models energy yes no no no yes
;
/solve/set time-step 0.001
/solve/set extrapolate-vars yes
; init statistics
/solve/init/init-flow-statistics
;
/define/boundary-conditions/wall tank-bottom 0 no 0 no yes heat-flux no 3000 no no no no 0 no 0.5
no 1
/solve/patch fluid-inner fluid-outer () temperature 300
; heat source to eliminate heating by heat flux through the walls, W/m3
; q = 3000
/define/parameters/input-parameters edit "heat-source" "heat-source" -74746.70976
; q = 30000
/define/parameters/output-parameters/print-all-to-console
/define/parameters/output-parameters/write-all-to-file params0.out
;
; auto-save every 1 s
/file/auto-save/data-freq 1000
/file/auto-save/append-file-name-with flow-time 6
/file/auto-save/retain-most-recent-files yes
/file/auto-save/max-files 1
/file/auto-save/root-name "autosave.gz"
; perform first set of iterations corresponding to ~ 5s
/solve/dual-time-iterate 4000 20
;
; define mean heat transfer coefficients, they are not defined before some statistics is collected
/define/parameters/output-parameters/create/surface-integral "mean-alpha" area-weighted-avg
mean-heat-transfer-coef tank-bottom tank-wall ()
```

/define/parameters/output-parameters/create/surface-integral "mean-alpha-bottom" area-weighted-avg mean-heat-transfer-coef tank-bottom ()

/define/parameters/output-parameters/create/surface-integral "mean-alpha-wall" area-weighted-avg mean-heat-transfer-coef tank-wall ()

;

; print all parameters to console

/define/parameters/output-parameters/print-all-to-console

/define/parameters/output-parameters/write-all-to-file params1.out

/file/write-case-data trans1-%t.cas.gz

;

; init statistics for the next set of time steps

/solve/init/init-flow-statistics

; perform another set of iterations/time steps

/solve/dual-time-iterate 16000 20

/exit yes.

7.2.1 Turbulence model

The k-ω based Shear-Stress-Transport (SST) turbulence model was chosen for our simulation of heat transfer in an agitated vessel. In chapter 5 briefly explained about k-ω SST turbulence model.

7.2.2 Material properties

The chosen fluid for simulation in an agitated vessel was 'water' (material) with constant thermo-physical properties from ANSYS Fluent database.
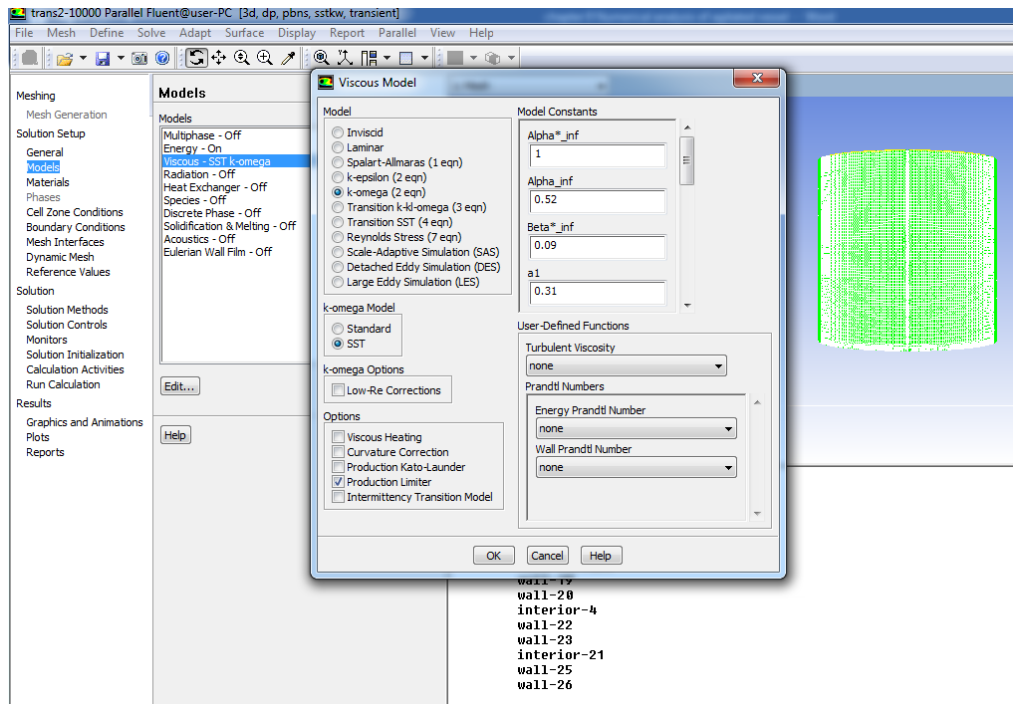
Figure 7.1: ANSYS Fluent 15.0 set up for different models.
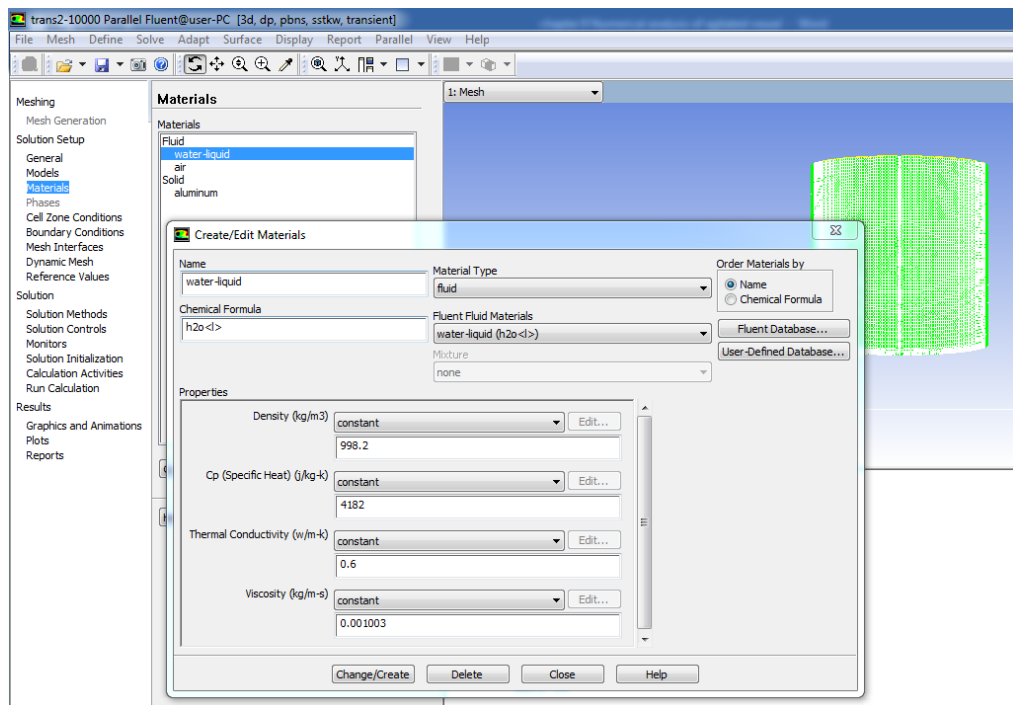
Figure 7.2: ANSYS Fluent 15.0 material properties set up with Fluent database.

7.2.3 Cell zone and Boundary conditions

In cell zone conditions, you can define the fluid parameter for inner and outer zones. In our case, the inner zone represents the region around the impeller with specific rotation speed, while the outer zone represented the agitated fluid domain with baffles which was kept stationary.

In chapter 5, we discussed the sliding mesh technique (Mesh motion) available in ANSYS Fluent. Simulations were performed using sliding mesh technique which set up is shown at Figure 7.3.
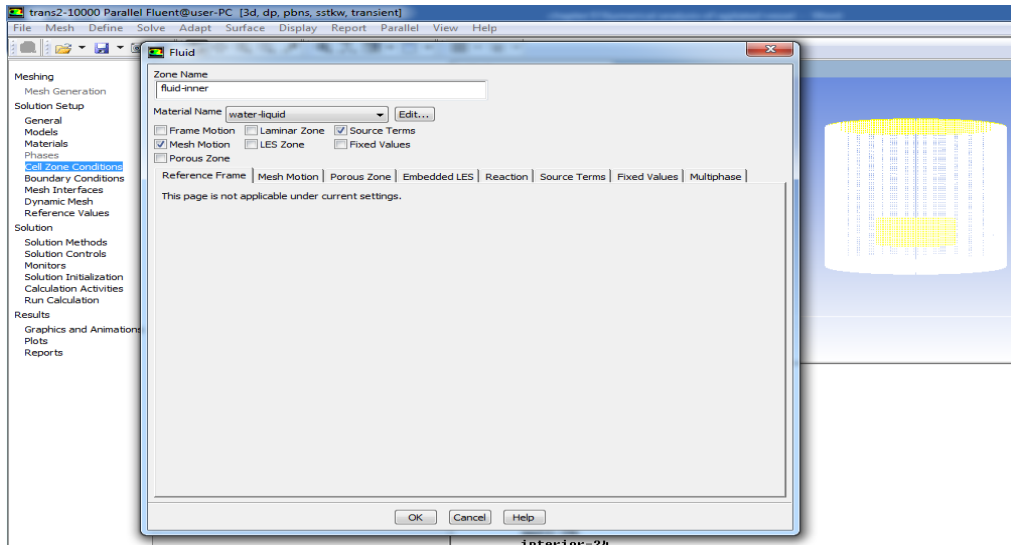
Figure 7.3: ANSYS Fluent 15.0 Cell zone with sliding mesh technique set up.

In cell zone conditions, energy sources can be applied that can act like heat sink in agitated vessel. Heat source (sink) was used to eliminate heating the liquid inside the vessel by heat flux through the walls. The value of heat source used in simulations was -74746.71 W/m^3. See the equation number [8.1] in chapter 8 more details.
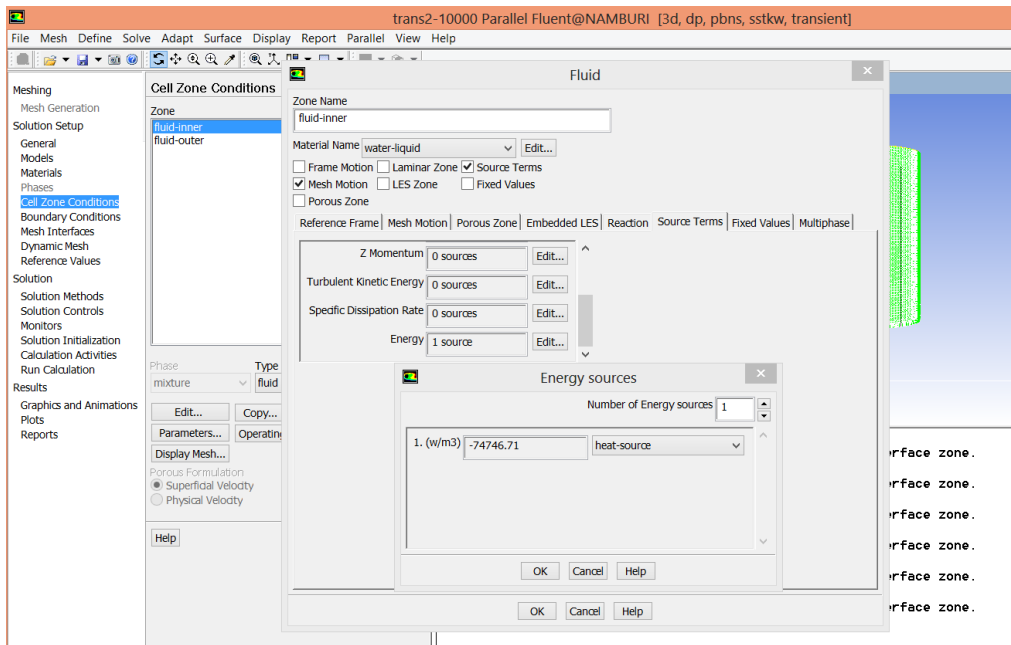
Figure 7.4: ANSYS Fluent 15.0 heat source set up.

Boundary conditions

Boundary conditions are parameters for running the simulations with appropriate material, thermal conditions, wall motion, shear conditions and wall roughness, etc. Figure 7.5 shows the ANSYS Fluent set up for thermal condition of constant heat flux with $q = 3000 \ W/m^2$

at tank-bottom and tank-wall which acts as heat supply. In the wall motion for impeller including shaft, 'moving wall' and 'no slip' were applied as shear condition.
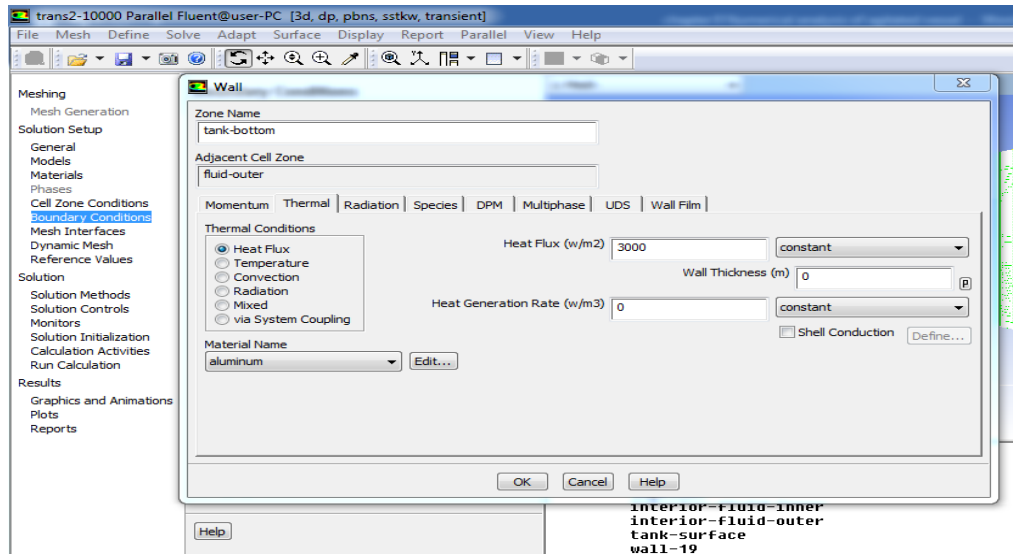
Figure 7.5: ANSYS Fluent 15.0 Boundary conditions set-up of heat flux.

7.2.4 Solution method

Solver type: Pressure based solver was selected for simulations in ANSYS Fluent. The first 2000 iterations were performed for steady state case to get a fully developed flow profile in the tank, then simulation was switched to transient model with energy equation on.

Solutions methods: Pressure-velocity coupling SIMPLE algorithm was chosen. Spatial Discretization: For momentum, turbulent kinetic energy, specific dissipation rate and energy second-order accurate upwind scheme was selected. Pressure: Standard, Gradient: Green-Gauss node based.

Run calculations: Time step size chosen 0.001 s, the maximum iterations per time step were 20 for all the simulations. Corresponding run-time for transient analysis was based on the mixing time t_m for different rotational speeds, see Table 4.2.
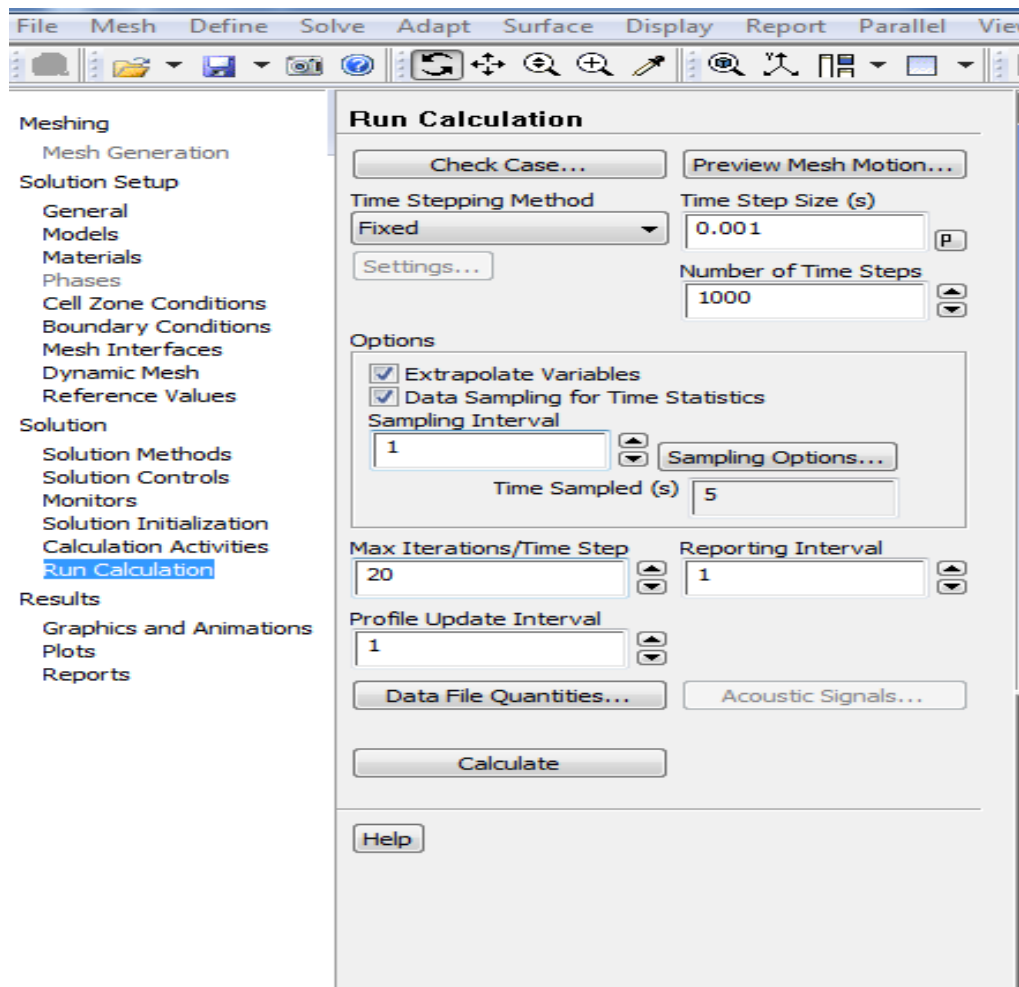
Figure 7.6: ANSYS Fluent 15.0 set up for solution methods.

7.3 Computational results

The post-processing results in ANSYS Fluent 15.0 for different range 300-900 rpm and off-bottom clearances h/d = 1, 2/3 ,1/3 cases were done. Here, some of velocity contours, temperature contours at bottom of agitated vessel and path lines are illustrated. The axial flow pattern developed by the PBT impeller inside the agitated vessel is clearly indicated here. In velocity contours plots for the off-bottom clearance h/d= 1, 2/3, 1/3, the light blue spots show dead zones of mixing.
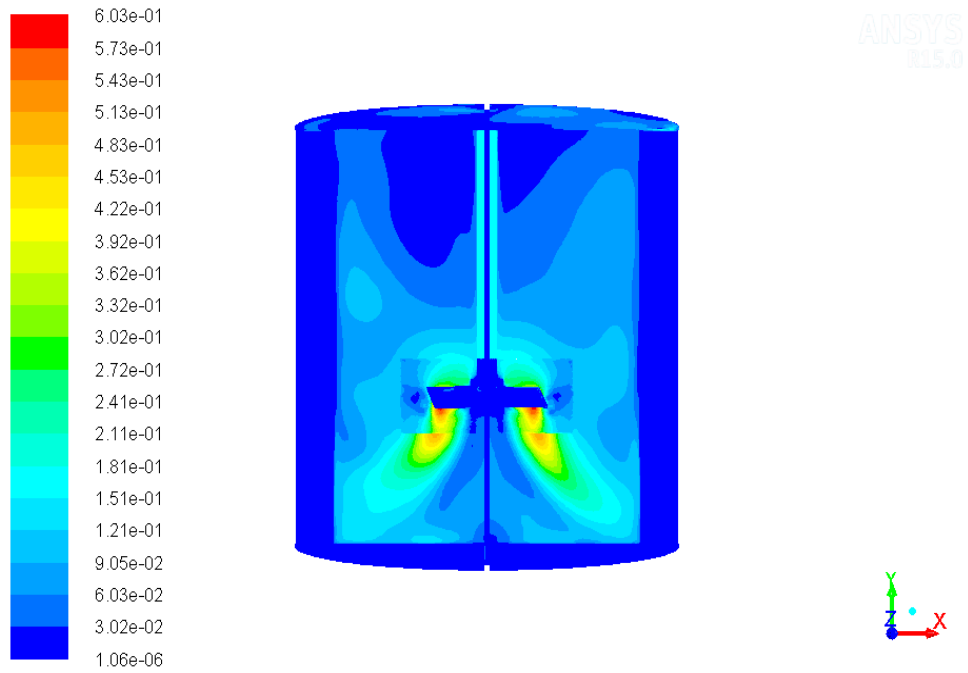
Figure 7.7: Velocity contours of agitated vessel off-clearance h/d= 1, 500 rpm.
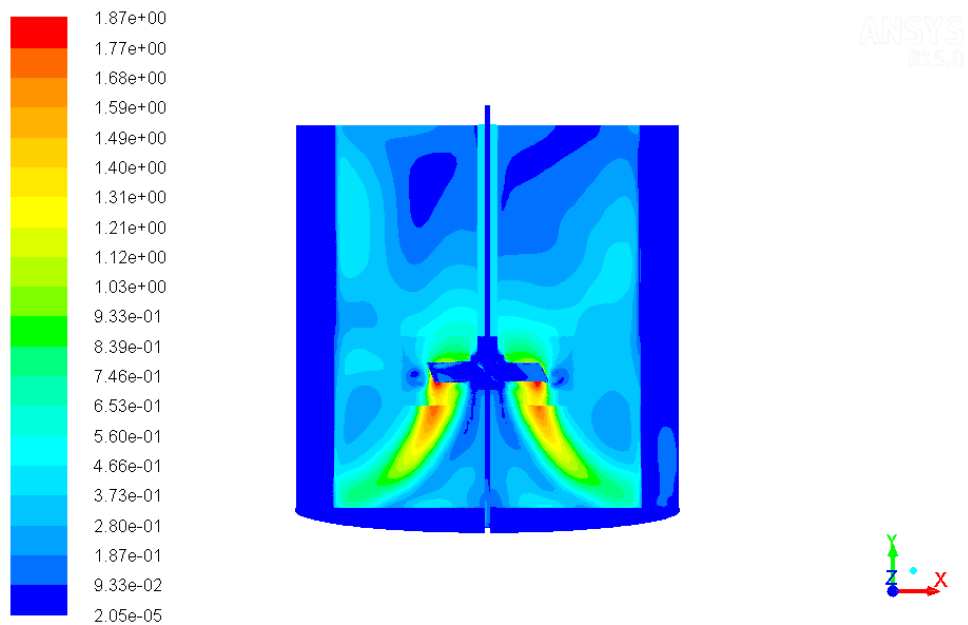
Figure 7.8: Velocity contours of agitated vessel off-clearance h/d= 1, 900 rpm.
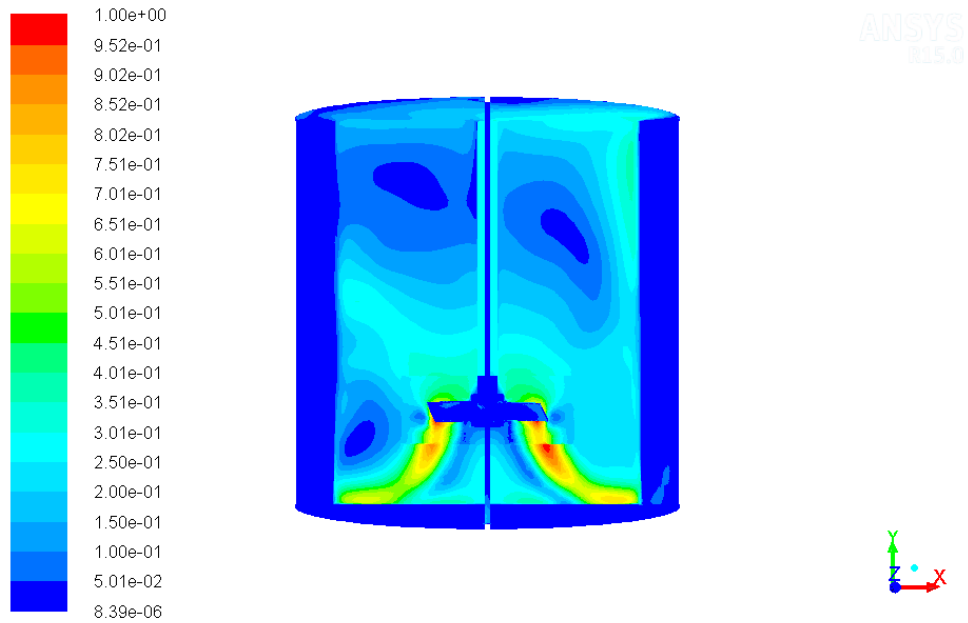
Figure 7.9: Velocity contours of agitated vessel off-clearance h/d= 2/3, 500 rpm.
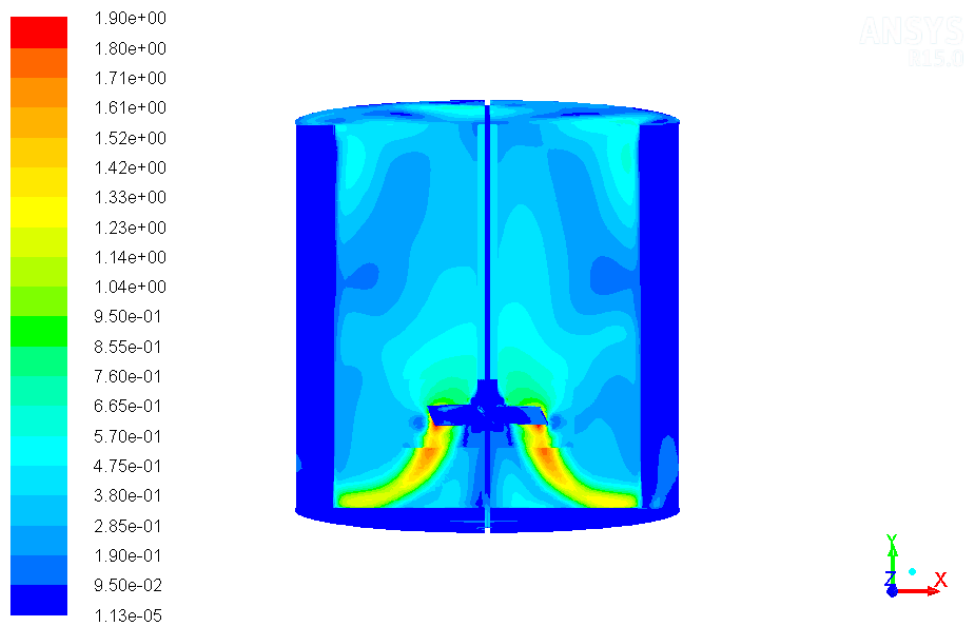
Figure 7.10: Velocity contours of agitated vessel off-clearance h/d= 2/3,900 rpm.
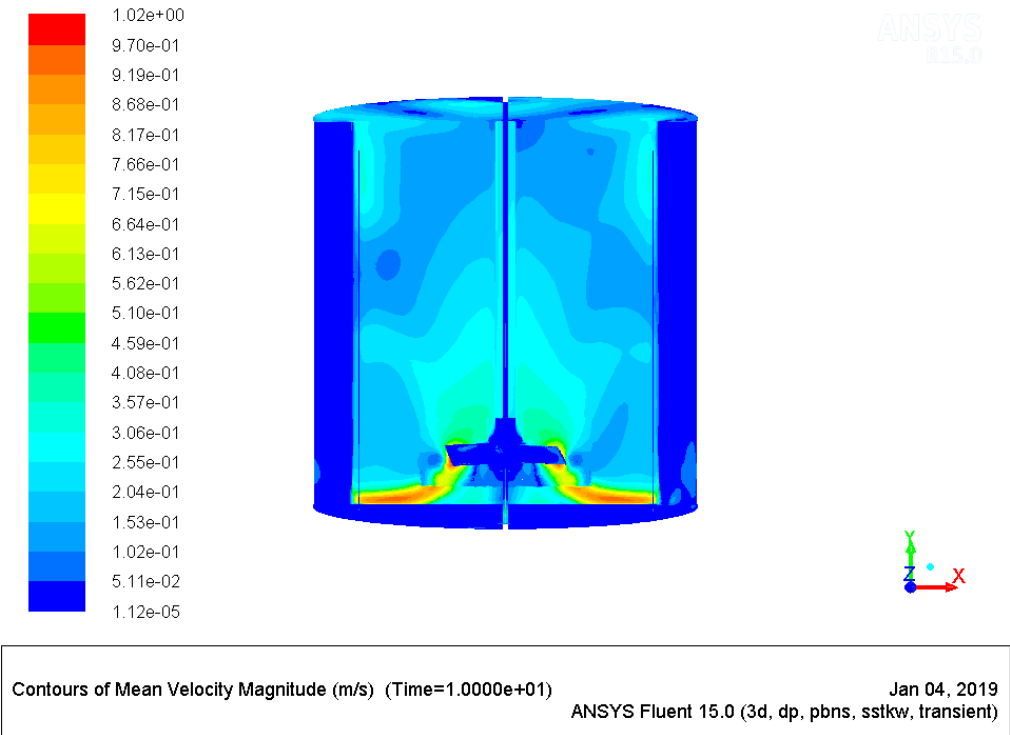
Figure 7.11: Velocity contours of agitated vessel off-clearance h/d= 1/3, 500 rpm.
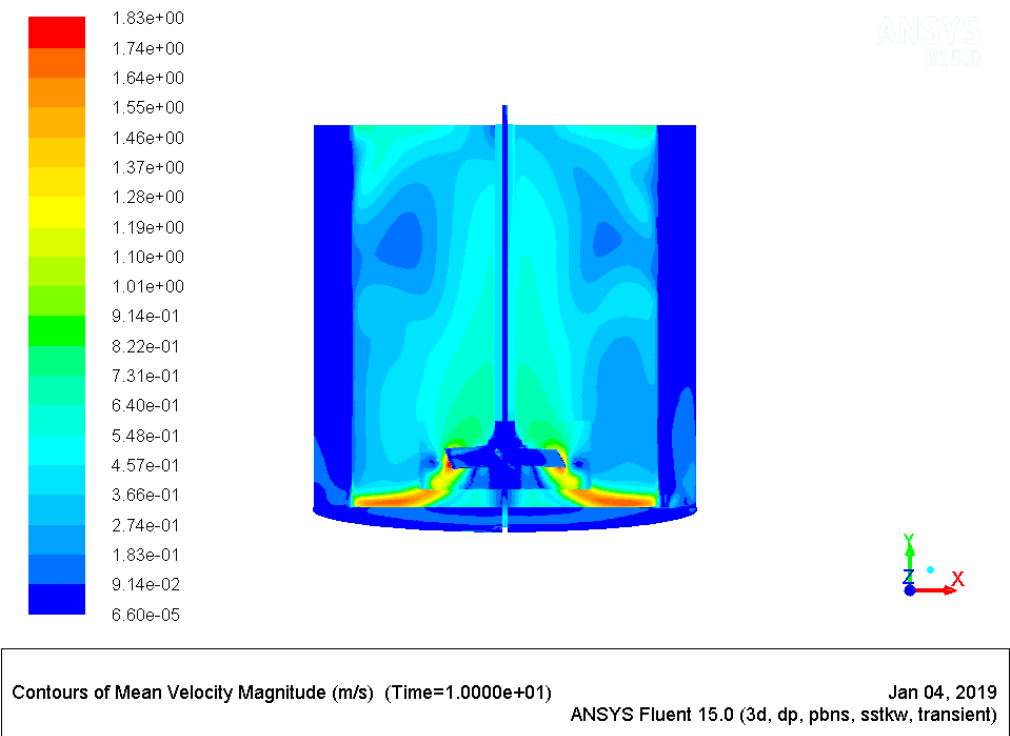
Figure 7.12: Velocity contours of agitated vessel off-clearance h/d=1/3, 900 rpm.
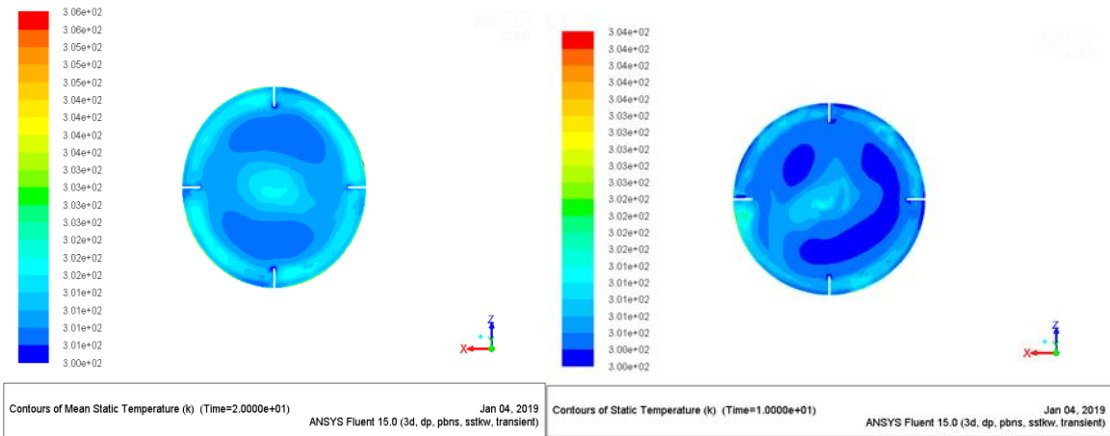
Figure 7.13: Contours of temperature at bottom of agitated vessel off-clearance h/d= 1, 500 rpm and 900 rpm.
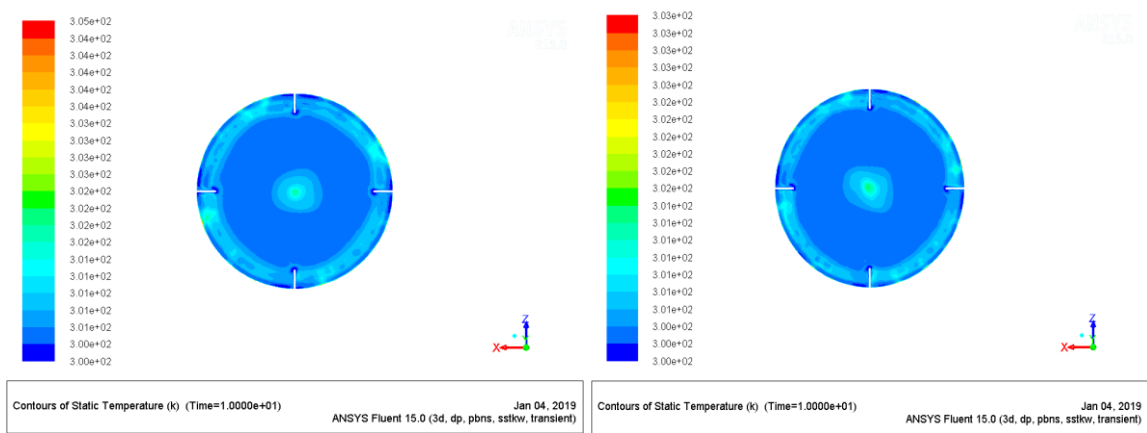
Figure 7.14: Contours of temperature at bottom of agitated vessel off-clearance 1/3, 500 and 900 rpm.
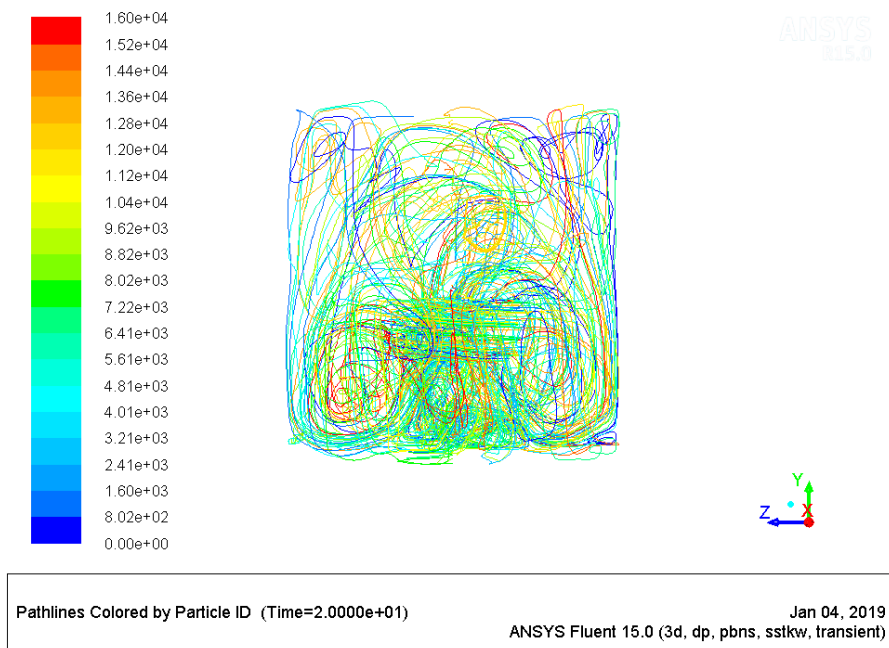
Figure 7.15: Pathlines illustrating flow pattern in the vessel for off-bottom clearance h/d=1, 500 rpm**.**

CHAPTER 8 SIMULATION RESULTS CORRELATION

8.1 Introduction

The theory of agitated vessel and heat transfer in agitated vessel was explained in chapter 2 and 3. Determining the heat transfer in agitated vessel can help in design and operation of batch or continuous reactor, for example. Heat transfer rate at the heat-exchange surface of agitated vessel should be sufficient to maintain the temperature inside the vessel within given range. One of the main objectives in this work was to determine heat transfer rate at the bottom, at the vertical walls, and at the whole heat exchange surface (bottom + wall) of agitated vessel. Analysis of impeller distance from bottom of vessel was also accomplished. The following section provide a brief overview of comparing the obtained results with available Nusselt number correlations in literature.

8.2 Heat transfer surfaces

In a jacketed agitated vessel, the steady state heat transfer is reached when temperature of the jacketed (bottom + walls) and batch reactor remains constant. It can be achieved when constant heat inlet (source) or outlet (sink) of system is balanced with the heat supplied or removed through the vessel jacket. The unsteady heat transfer of system occurs when the temperature of the batch changes during the agitation (exothermic or endothermic) from initial to final temperatures.

8.3 Solution procedure

In present work, CFD simulation of transient (time-dependent) heat transfer in an agitated vessel was studied with a pitched six-blade turbine impeller with supplying constant heat flux $q = 3000\,\text{W/m}^2$ at the wall and bottom of the vessel. Initial temperature was set at 300 K inside the agitated vessel. During the agitation of fluid in tank, the temperature of the system would increase by supplying the heat flux to the system. To prevent the temperature change of the fluid in the agitated vessel, heat sink was used in the simulations. Its value $\dot{Q}^{(g)}$ was based on the following equation.

$$q\,S = \dot{Q}^{(g)}\,V \qquad\qquad [8.1]$$

$$\dot{Q}^{(g)} = \frac{-q * S}{V} \qquad\qquad [8.2]$$

where $\dot{Q}^{(g)}$ is heat sink.

In this case, q = 3000 W/m² , surface area S = 0.157, volume of the tank V =0.0068 m^3. Substituting the values in equation [8.1], $\dot{Q}^{(g)}$ = -74746.71 W/m³. Using the heat sink will help to avoid the necessity of a correction for the fluid temperature see, (Chakravarty, 2017) for more details.

In one of the cases the CFD simulation of agitated vessel at 500 rpm was done for the constant heat flux q = 3000 W/m²and it was compared with 10-time greater value q = 30000W/m². The Fluent results for mean heat transfer coefficient did not vary too much, the value were almost same, and all consequent simulations were performed with q = 3000 W/m². Table 8.1 shows values of ANSYS Fluent output. Simulations were done for 500 rpm and different heat flux q = 3000 W/m² and q = 30000 W/m².

Output Parameter	Value units
Temperature	3.000e+02 K
Mean-Alpha	3.404e+03 W/m²K
Mean-Alpha-Bottom	5.101e+03 W/m²K
Mean-Alpha-Wall	2.976e+03 W/m²K

Table 8.1: Heat flux q = 3000 W/m², 500 rpm output values.

Output Parameter	Value units
Temperature	3.000e+02 K
Mean-Alpha	3.404e+03 W/m²K
Mean-Alpha-Bottom	5.101e+03 W/m²K
Mean -Alpha-Wall	2.976e+03 W/m²K

Table 8.2: Heat flux q = 30000 W/m², 500 rpm output values.

8.4 Correlations for the Nusselt number

After ANSYS Fluent simulation for 15 different rotational speeds ranging from 300 rpm to 900 rpm and varying off-bottom clearance of h/d =1, 2/3, 1/3 of impeller were performed. The values of mean Nusselt number (bottom + wall), mean Nusselt number (bottom), mean Nusselt number (wall) were evaluated at the end of simulations. Table 8.3 shows the mean values of Nusselt numbers and corresponding Reynolds number, which were calculated from equations [3.2] and [3.3]. For all the parameters of the calculation values can the reader can refer to Appendix C.

CASE 1: Distance h/d = 1 off bottom-clearance of impeller.

Impeller rotational speed (rpm)	Reynolds Number, Re	Mean Nusselt Number		
		Bottom+wall	Bottom	Wall
300	22116	660.711	908.063	598.399
500	36860	952.525	1349.346	852.560
700	51604	1310.961	1824.793	1181.519
900	66348	1687.206	2267.020	1541.142

Table 8.3: Values of Nusselt and Reynolds number according to the rotational speeds

CASE 2: Distance h/d= 2/3 off bottom-clearance of impeller.

Impeller rotational speed (rpm)	Reynolds Number, Re	Mean Nusselt Number		
		Bottom+wall	Bottom	Wall
300	22116	735.966	1127.500	637.333
400	29488	932.660	1408.892	812.690
500	36860	1134.701	1700.521	992.162
500 ($q = 3000$ W/m^2)	36860	1134.694	1700.500	992.159
600	44232	1309.172	1934.040	1151.758
700	51604	1548.293	2213.601	1380.692
800	58976	1716.432	2463.305	1528.284
900	66348	1953.621	2722.939	1759.819

Table 8.4: Values of Nusselt and Reynolds number according to the rotational speeds.

CASE 3: Distance h/d =1/3 off bottom-clearance of impeller.

Impeller Rotational speed (rpm)	Reynolds Number, Re	Nusselt Number		
		Bottom+wall	Bottom	Wall
300	22116	860.955	1279.885	755.421
500	36860	1298.673	1921.520	1141.769
700	51604	1718.972	2489.763	1524.799
900	66348	2245.243	3027.882	2048.085

Table 8.5: Values of Nusselt and Reynolds number according to the rotational speeds.

Heat transfer correlation of Nusselt number Nu is usually expressed as a combination of dimensionless groups in the form described in detailed in chapter 3.

Our aim was to present a correlation for the Nusselt number as follows:

$$\mathrm{Nu} = C\ \mathrm{Re}^a\ \mathrm{Pr}^b\ \mathrm{Vi}^c\ \mathrm{G_c} \qquad [8.3]$$

Using MATLAB function nlinfit, a nonlinear regression was performed to calculate the coefficients of leading constant C and power a. For MATLAB scripts, refer to Appendix D.

From literature, correlations were found to compare the ANSYS Fluent results of heat transfer in an agitated vessel with fluid of constant Prandtl number equal to 7.021(water). Temperature-dependence of thermophysical properties of process fluid was neglected, and Reynolds number range was $7\ X\ 10^4 < \mathrm{Re} < 7\ X\ 10^5$. The experimentally obtained heat transfer correlation for pitched blade turbine PBT impeller in baffled vessels developed by (Chapman et al., 1964) is

$$\mathrm{Nu} = 0.74\ \mathrm{Re}^{\frac{2}{3}}\mathrm{Pr}^{\frac{1}{3}}\ \mathrm{Vi}^{0.14}\left(\frac{S_{bl}/Di}{1/5}\right)^{0.2}\left(\frac{N_{bL}}{\sigma}\right)^{0.2}[\sin(\theta)]^{0.5} \qquad [8.4]$$

where S_{bl} is width of the blade, D_i is impeller dimeter, N_{bl} is number of blades and θ is pitch angle of blade. For our geometrical specification, $S_{bl} = 0.02$, $N_{bl}= 6$ and $\theta = 45°$. This Chapman correlation was compared with our results for off-bottom clearance of h/d= 2/3 (impeller distance from the bottom of vessel) (Chisholm et al., 1988).

Nagata et al. (1972) published the following equation for the Nusselt number in a stirred vessel baffled fitted with the pitch blade impeller and baffles (VDI Heat Atlas, 1993).

$$\mathrm{Nu} = 1.4\left(\frac{d_R}{d_B}\right)^{0.3}\left(\frac{h}{d_B}\right)^{0.45}\left(\frac{h_R}{h_L}\right)^{0.2}\left(\frac{h_L}{d_B}\right)^{-0.6}\sin(\gamma)^{0.5}\ Z^{0.2}\ \mathrm{Re}^{\frac{2}{3}}\mathrm{Pr}^{\frac{1}{3}}\left(\frac{\eta}{\eta_\omega}\right)^{0.14} \qquad [8.5]$$

where impeller diameter to vessel diameter $\frac{d_R}{d_B} = \frac{1}{3}$, ratio of liquid height to vessel diameter $\frac{h_L}{d_B} = 1$, ratio of height of impeller above bottom to liquid height $\frac{h_R}{h_L} = \frac{1}{3}$, ratio of baffles width to vessel diameter $\frac{b_s}{d_B} = \frac{1}{10}$, number of baffles $n_s = 4$. In our case we are comparing the results for off-bottom clearance h/d = 1 and h/d =1/3 impeller with Nagata el al. (1972) correlation.

Table 8.6 shows the value of the coefficients C and a their confidence intervals regions which best fit values of mean Nusselt number (Bottom +Wall), bottom and wall. It is for case h/d= 2/3 off-bottom clearance.

Nusselt Number	C	Confidence interval of C	Percentage %	a	Confidence interval of a	Percentage %
Bottom + wall	0.045	±0.025	56%	0.90	±0.052	5.79%
Bottom	0.184	±0.042	22.8%	0.80	± 0.021	2.62%
Wall	0.126	± 0.246	195%	0.78	±0.181	23%

Table 8.6: Values of the coefficients for the correlation of Nusselt number, off-bottom h/d=2/3.

The resulting correlations can be summarized as follows:

$$\text{Nu}_{\text{bottom+wall}} = 0.045 \ \text{Re}^{0.90} \ \text{Pr}^{0.33} \qquad [8.6]$$

$$\text{Nu}_{\text{bottom}} = 0.184 \ \text{Re}^{0.80} \ \text{Pr}^{0.33} \qquad [8.7]$$

$$\text{Nu}_{\text{wall}} = 0.126 \ \text{Re}^{0.78} \ \text{Pr}^{0.33} \qquad [8.8]$$

Equations [8.6], [8.7] and [8.8] represent the heat transfer correlations obtained by the ANSYS Fluent evaluation of unsteady heat transfer with flat bottom agitated vessel mounted with six blade PBT impeller. Exponent 'b' of Pr was kept as 0.33 and Vi was completely neglected. The obtained heat transfer correlations were compared with the experimental work of Chapmen et al. (1964) and Nagata et al (1964). Figure 8.1, 8.2, and 8.3 shows the relation between Nusselt number and Reynolds number, obtained data and fitted correlations compared with the experiment work of Chapman et al. (1964) and Nagata et al. (1972).
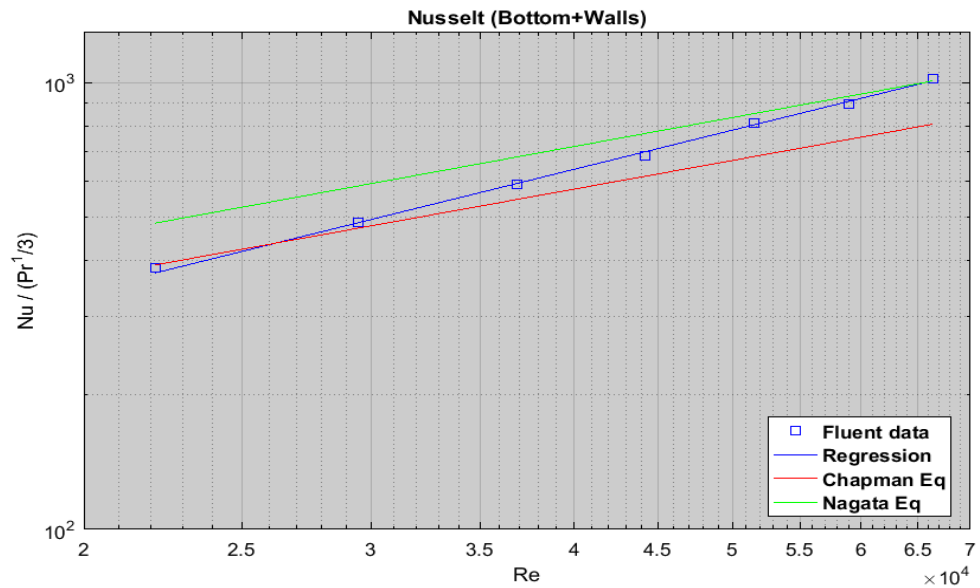
Figure 8.1: Obtained data and fitted correlations compared Nusselt (bottom + wall) with the experiment work of Chapman et al. (1964) and Nagata et al. (1972).
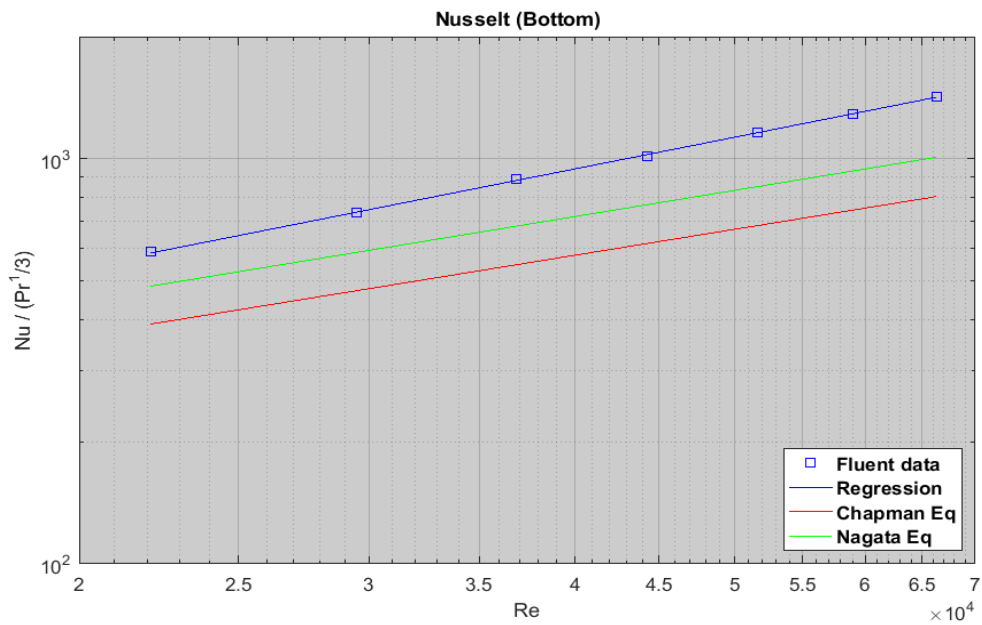
Figure 8.2: Obtained data and fitted correlations compared Nusselt (bottom) with the experiment work of Chapman et al. (1964) and Nagata et al. (1972).
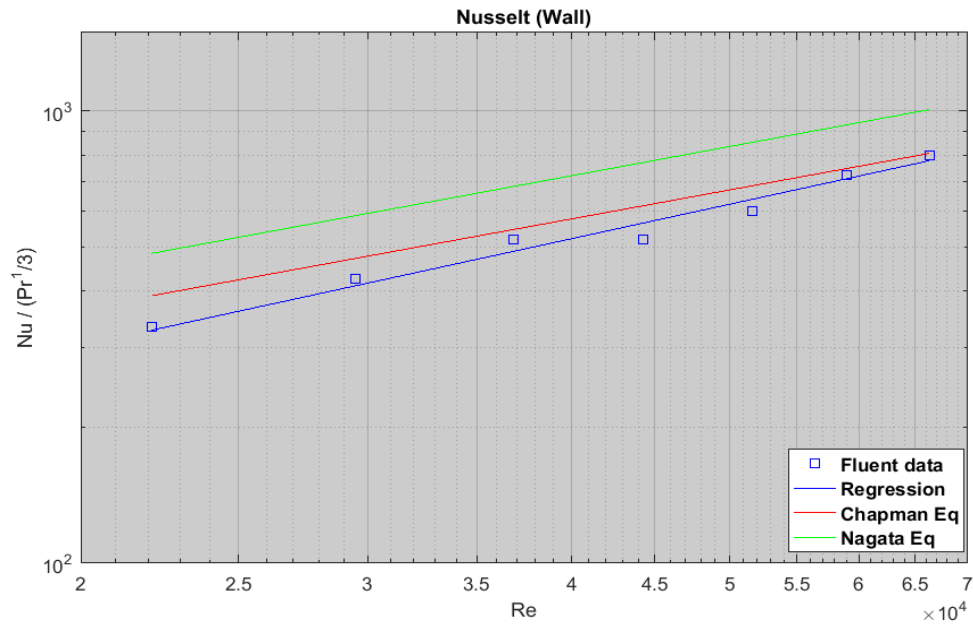
Figure 8.3: Obtained data and fitted correlations compared Nusselt (wall) with the experiment work of Chapman et al. (1964) and Nagata el at. (1972).

We can observe from Table 8.6 the coefficients *C* are much smaller when comparing with experiment work of Chapman et al. (1964) correlation. This is a consequence of substantially higher value of parameter *a*. The confidence intervals of *C* are also high especially for the wall. For this reason, another nonlinear regression was performed to compare the results of with correlation of Chapman, but this time only constant *C* was calculated and the exponent of Reynolds number *a* was fixed as commonly used value 0.66. For MATLAB script the reader can refer to Appendix E.

Nusselt Number	*C*	Confidence interval of C	Percentage %
(Bottom + wall)	0.57	±0.040	7.09%
Bottom	0.82	±0.035	4.23%
Wall	0.45	±0.026	5.8%

Table 8.7: Values of the parameter *C* in the correlation coefficients for Nusselt number with fixed of exponent of Reynolds number used 0.66 case off-bottom clearance h/d = 2/3.

The resulting correlations can be summarized as follows:

$$Nu_{bottom+wall} = 0.57 \ Re^{0.66} \ Pr^{0.33} \qquad [8.9]$$

$$Nu_{bottom} = 0.82 \ Re^{0.66} \ Pr^{0.33} \qquad [8.10]$$

$$\mathrm{Nu_{wall}} = 0.45\ \mathrm{Re}^{0.66}\ \mathrm{Pr}^{0.33} \qquad\qquad [8.11]$$
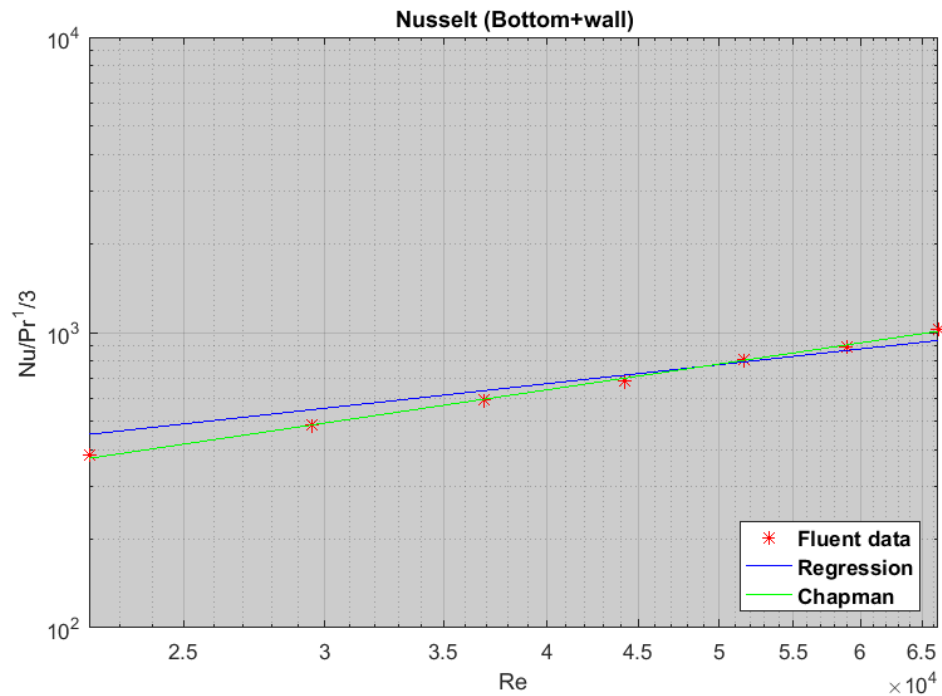
Figure 8.4: Obtained data and fitted correlations compared Nusselt (wall) with the experiment work of Chapman et al. (1964).

In present work we varied off-bottom clearance of impeller h/d = 1 and h/d = 1/3 from bottom of tank. From the literature, Nagata et al. (1972) correlation (equation [8.5]) takes into account the impeller distance from the bottom and can be used for comparison. Table 8.8 shows the values of evaluated coefficients C and a with their confidence intervals for Nusselt (bottom + wall), Nusselt bottom, Nusselt wall for off-bottom clearance of h/d =1 shows the values and Table 8.9 shows these coefficients for off-bottom clearance h/d = 1/3.

Nusselt Number	C	Confidence interval of C	a	Confidence interval of a
Bottom+ wall	0.042	±0.106…. (250%)	0.89	±0.23…. (25%)
Bottom	0.094	±0.090…. (95%)	0.84	±0.87…. (%10.35)
Wall	0.031	±0.099… (300%)	0.91	0.28 … (31 %)

Table 8.8: Values of the coefficients for the correlation of Nusselt number, case off- bottom clearance h/d = 1.

The correlation can be summarized as follows:

$$\mathrm{Nu_{bottom+wall}} = 0.042 \ \mathrm{Re}^{0.89} \ \mathrm{Pr}^{0.33} \qquad [8.7]$$

$$\mathrm{Nu_{bottom}} = 0.094 \ \mathrm{Re}^{0.84} \ \mathrm{Pr}^{0.33} \qquad [8.8]$$

$$\mathrm{Nu_{wall}} = 0.031 \ \mathrm{Re}^{0.91} \ \mathrm{Pr}^{0.33} \qquad [8.9]$$

Nusselt Number	C	Confidence interval of C	a	Confidence interval of a
Bottom + wall	0.056	±0.126 …. (223%)	0.89	± 0.205 …. (23%)
Bottom	0.272	± 0.053 … (19%)	0.78	± 0.017… (2.30%)
Wall	0.030	± 0.079 …. (318%)	0.94	±0.292 … (31 %)

Table 8.9: Values of the coefficients for the correlation of Nusselt number, case off-bottom clearance h/d =1/3.

The correlation can be summarized as follows:

$$\mathrm{Nu_{bottom+wall}} = 0.056 \ \mathrm{Re}^{0.89} \mathrm{Pr}^{0.33} \qquad [8.10]$$

$$\mathrm{Nu_{bottom}} = 0.272 \ \mathrm{Re}^{0.78} \mathrm{Pr}^{0.33} \qquad [8.11]$$

$$\mathrm{Nu_{wall}} = 0.030 \ \mathrm{Re}^{0.94} \mathrm{Pr}^{0.33} \qquad [8.12]$$
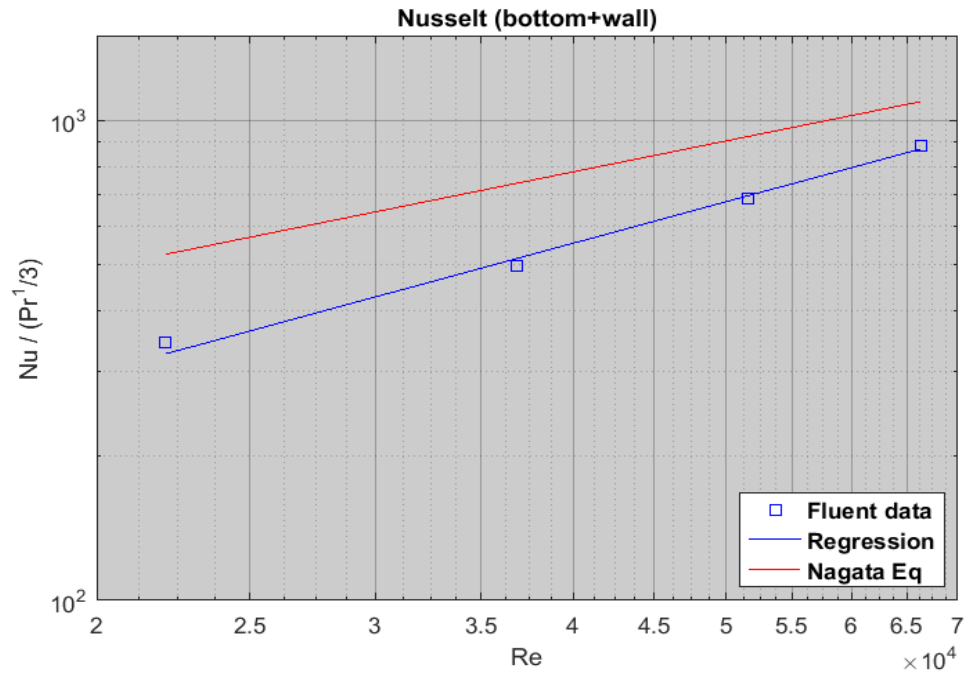
Figure 8.5: Obtained data and fitted correlations compared Nusselt (bottom + wall), with the experiment work of Nagata et al. (1972), off-bottom clearance h/d = 1.
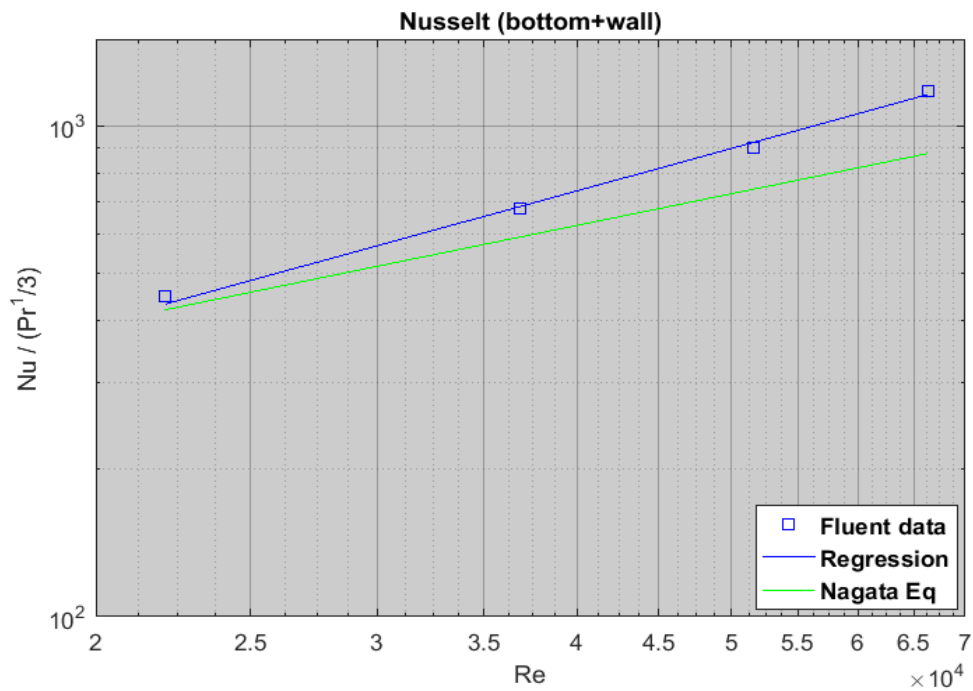
Figure 8.6: Obtained data and fitted correlations compared Nusselt (bottom + wall), with the experiment work of Nagata et al. (1972), off-bottom clearance h/d = 1/3.

The value of *C* leading constant depends mainly upon geometry of the system (standard or nonstandard geometry) and the type of impeller, number of blades and angle of blade and geometry of agitated vessel with round or flat bottom head. In our results, the values of *C* and '*a*' of Re have very large confidence intervals. To improve it, more simulations for other

speeds should be run, so that more data points could be obtained for off-bottom clearances h/d=1 and h/d =1/3. Another improvement could lie in increasing the simulation run-time and reducing time step size.

The influence of impeller distance from bottom for vessel for all h/d = 1, 2/3 and 1/3 cases were evaluated in MATLAB regression.

The correlation can be summarized as follows for h/d = 1, 2/3, 1/3

$$\text{Nu}_{\text{bottom+wall}} = 0.043 \, \text{Re}^{0.89} \, \text{Pr}^{0.33} \left(\frac{h}{d}\right)^{-0.24} \qquad [8.13]$$
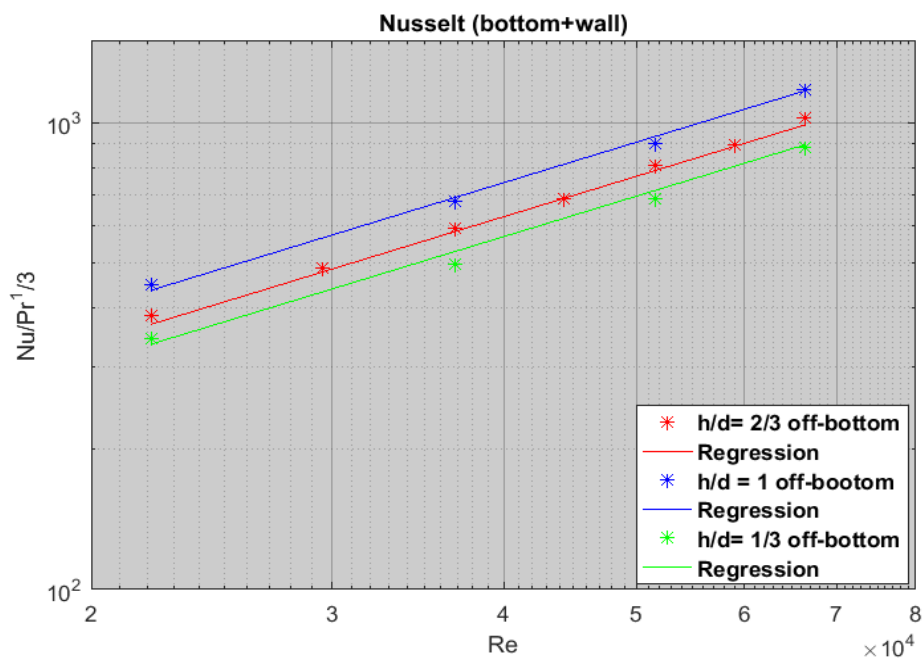
Figure 8.7: Obtained data and fitted correlations compared Nusselt (bottom + wall), off-bottom clearance h/d = 1, 2/3, 1/3.

Nusselt Number	C	Confidence interval of C	a	Confidence interval of a	$\dfrac{h}{d}$	Confidence Interval of $\dfrac{h}{d}$
Bottom + wall	0.043	± 0.026 … (60 %)	0.89	± 0.055 … (6.19%)	-0.24	± 0.039 … (16 %)
Bottom	0.170	± 0.141… (82.88)	0.80	± 0.076… (9.56%)	-0.25	± 0.056… (22%)
Wall	0.025	± 0.016…. (63%)	0.93	± 0.058… (6.23%)	-0.23	±0.040 … (16.9%)

Table 8.10: Values of the coefficients for the correlation of Nusselt number, case off-bottom clearance h/d = 1, 2/3, 1/3.

From the observation of evaluated data, velocity and temperature contours, it can be concluded that the influence of impeller moving towards the bottom of the vessel, heat transfer rate is slightly increasing, and at wall of the vessel it is slightly decreasing. It is similar to impinging jet (Petera et al., 2017).

8.5 Verification of final temperature analytically

The final temperature can be calculated analytical and compared with results of ANSYS Fluent simulation.

Equation to calculate the heat flux:

$$Q = m \, c_p \frac{dT}{dt} \qquad [8.14]$$

where m is total mass of the heated fluid, which can be calculated as the volume of the tank times the density of the water [998.2 Kg/m^3]. The specific heat capacity (C_p) is 4182 [J/Kg K]. With heat flux of q= 3000 W/m^2 , we need to consider the surface area where heat flux is applied bottom and wall of agitated vessel [S]. Therefore, the previous equation [8.14] can be written as:

$$q \, S = V_{tank} \, \rho_{water} \, Cp_{water} \, \frac{dT}{dt} \qquad [8.15]$$

This is an ordinary differential equation, which can be solved by separating the variables and integration. The limits for integration for the temperature side are initial temperature, which is known T_w = 300 K and final temperature T_f, mixing time t_m = 0 to 20 seconds.

$$q \, S \int_{0}^{20} dt = V \, \rho \, Cp \int_{300}^{T_f} dT$$

$$q \, S \, (20 - 0) = V \, \rho \, Cp \, (T_f - 300)$$

$$T_f = \frac{q \, S \, (20)}{V \, Cp \, \rho} + 300 \, K \qquad [8.16]$$

There the surface (S), can be calculated as the sum of the bottom surface [$\pi \, r^2$] and the wall surface [$2 \, \pi \, r^2 \times H$]. The diameter of tank 0.2 m and the height is 0.2 m, total surface $S = 0.157 \, m^2$ and volume of the tank ($\pi r^2 \times H$) is 0.0068 m^3 by calculating the values in

equation [8.16] the final temperature T_f is 300.33 K, whereas temperature obtained from volume integrals method from the simulation is 300.01 K. Which confirms that the calculations are correct.

For calculation of the heat transfer coefficient, ANSYS Fluent solver does consider this increase, but takes the temperature of the fluid as constant input parameter (T_{ref}) according to the following equation:

$$\alpha = \frac{q}{T_{ref} - T_w} \qquad [8.17]$$

where q is heat flux and T_w is temperature at the wall. That is why internal sink of heat was used in all simulations so that the fluid temperature would not change substantially (section 8.3).

9. CONCLUSION AND FUTURE SCOPE

9.1 Conclusions

The following conclusion have been drawn in this master thesis:

a) A literature research was done to find the scientific works related to the heat transfer in an agitated vessel with pitched blade turbine impeller

b) Geometry of agitated vessel and meshing

    i.   Three-dimensional geometry of agitated vessel was created by using ANSYS Workbench15.0 for three different cases of off-bottom clearance h/d = 1, 2/3, 1/3 (distance of impeller from the bottom).

   ii.   To improve the mesh quality, conversion of tetrahedral mesh elements to polyhedral were done in ANSYS Fluent.

 iii.   The power characteristics of the PBT impeller was compared with experiment work of Beshay et al. (2001).

  iv.   Sliding mesh technique has been used.

c) The heat transfer coefficients of transient simulation of agitated vessel

    i.   The solution strategy for the ANSYS Fluent solver was based on performing unsteady simulations during heating of batch of liquid.

   ii.   Three dimensional simulations of heat transfer fluid flow have been performed using k-ω (SST) turbulence model.

 iii.   Internal heat source (sink) was used to eliminate the change of fluid temperature caused by constant heat flux at bottom and vertical walls of agitated vessel.

  iv.   Two different simulations for constant heat flux $q = 3000 \ W/m^2$ and $q = 30000 W/m^2$ for rotational speed of impeller 500 rpm were performed to verify its influence. It was negligible.

   v.   The simulation for the impeller distance from the bottom h/d= 1, 2/3, 1/3, constant heat flux $q = 3000 W/m^2$ and rotational speeds from 300 to 900 rpms were performed.

  vi.   The heat transfer coefficients and mean Nusselt numbers at bottom + wall, bottom only and wall only were evaluated in ANSYS Fluent 15.0. Heat transfer correlations for Nusselt numbers were developed using non-linear analysis (nlinfit2) in MATLAB.

vii. The developed correlations were compared with the experimental work of Chapman et al. (1964) for case off-bottom clearance h/d= 2/3, and Nagata et al. (1972) for case off-bottom clearance h/d= 1, 1/3.

viii. The impact of the off-bottom clearance was described by the correlation for the Nusselt number. In general, the smaller is the distance the larger is the heat transfer rate which is in accordance with the negative power of h/d term in the correlation. It is similar to impinging jet case.

9.2 Future Scope

This work was focused on heat transfer simulation which could be used in optimising the agitated vessel design with different rotational speed of impeller. In addition to this work the following can be done in future:

- By increasing the run time simulation Δt_m and decreasing the time step, more accurate results might be obtained.

- Simulation based on other turbulence models like LES (Large eddy simulation) and RSM (Reynolds Stress Model) with fine mesh quality could also provide better results. On other side, much larger computational requirements would needed be and as well as more number of simulations days.

- In present work, baffled vessel with flat bottom is used. In food processing industries, round bottom is more frequently used which could be done in another simulations.

- The influence of thermos-physical properties of fluid and Prandtl number (Pr), and other types of impeller like Rushton disk turbine can be considered for the same geometry.

REFERENCES

1. ANSYS 13.0 Training material, 2010.

2. ANSYS 15.0 Training material, 2014.

3. ANSYS 6.1 Fluent User's Guide, ANSYS, Inc, 2003.

4. Bakker, A., Laroche, R.D, Wang, M.H and Calabrese, R.V.: Sliding Mesh Simulation of Laminar Flow in Stirred Reactors, *Chemical Engineering Research and Desig*, v.75, pp. 42-44, 1997.

5. Beshay, K.R., Kratěna, J., Fořt, I, Brůha, O.: Power Input of High Speed Rotary Impellers. *Acta Polytechnica,* v. 41 (6), pp. 18-23, 2001.

6. Brodkey, R.S., Hershey, H.C.: *Transport Phenomena: a unified approach,* McGraw-Hill Book Co. pp. 359-396, 1988.

7. Brenner, G.: CFD in Process Engineering,' Notes on Num.Fluid Mech., Springer, v 100, pp. 351-359, 2009.

8. Celik, I.B., Ghia, U., Roache, P.J., Freitas, C.J., Coleman, H., Raad, P.E.: Procedure for Estimation and Reporting of Uncertainty due to Discretization in CFDs applications, *Journal of Fluids Engineering*, 130, 2008.

9. Chakravarty, A.: CFD Simulation of Heat Transfer in an Agitated Vessel, Master Thesis, 2017.

10. Chisholm, D., ed. *Heat Exchanger Technology*, Elsevier Applied Science, pp.157-186, 1998.

11. Dostál, M., Petera, K, Rieger, F.: Measurement of Heat Transfer Coefficients in an Agitated Vessel with Tube Baffles, *Acta Polytechnica,* v.50 (2), pp. 46-57, 2010.

12. Incropera, F. P., DeWitt, D. P., Bergman, T. L., Lavine, A. S.: Fundamentals of Heat and Mass Transfer, 7th edition, Wiley, 2007.

13. McCabe, W. L., Smith, J. C., Harriott, P.: Unit Operations of Chemical Engineering, *McGraw-Hill Book Co.*, pp 235-281, 1993.

14. Novák, V., Rieger, F., Vavro, K.: Hydraulicke pochody v chemickem a potravinarskem prumyslu, SNTL, Praha, 1989.

15. Paul, E. L., Atiemo-Obeng, V. A, Kresta, S. M.: *Handbook of Industrial Mixing*, New Jersey, John Wiley, and Sons, 2003.

16. Petera, K., Dostál, M., Věříšová, M., Jirout, T.: Heat transfer at the bottom of a cylindrical vessel impinged by a swirling flow from an impeller in a draft tube. *Chem. Biochem. Eng.*, v. 31(3). pp 343-352, 2017.

17. Singh, H.: CFD Simulation of turbulent heat transfer in an agitated vessel, Master thesis, 2014.

18. Torotwa, I., Changying J.: A Study of Mixing Performance of Different Impeller Designs in Stirred Vessels using Computational Fluid Dynamics. *Journal MDPI Designs*, v. 8, 2018.

19. VDI Heat Atlas, editor P. Stephan, 2nd edition, Springer, 1993.

20. Versteeg, H. K., Malalasekera, W.: An Introduction to Computational Fluid Dynamics the Finite Volume Method, 2nd edition, 2007.

List of Figures

List of Tables

Nomenclature

Dimensionless number

Re   Reynolds number [-]
a exponent of Reynolds number
Pr   Prandtl number [-]
b   exponent of Prandlt number
c   exponent viscosity correction factor
Nu   Nusselt number [-]
Po   Power number [-]
Vi viscosity ratio [-]
C leading constant
S   swirl number
G_d geometri correction factor [-]
nt_m dimensional rotation speed[-]

Turbulence modelling

K turbulent kinetic energy [$m^2\ s^{-2}$]
ε kinetic energy dissipation rate [$m^2\ s^{-3}$]
ω specific dissipation rate [s^{-1}]
u' fluctuating velocity [$m\ s^{-1}$]
U actual velocities [$m\ s^{-1}$]
μ_t turbulent viscosity [$m^2\ s^{-1}$]
$\overline{U}$ time average of velocity (mean velocity)[$m\ s^{-1}$]
ϕ velocity component [s^{-1}]
$\vec{u}$ flow velocity [$m^3\ s^{-1}$]
$\vec{\vec{\tau}}$ stress tensor [$N\ m^{-2}$]
$\vec{f}$ body force [N]
$\tilde{G}_k$ generation of turbulent kinetic energy[$J\ kg^{-1}$]
$\vec{\vec{\Delta}}$ velocity gradient [s^{-1}]
u velocity of the flow[$m\ s^{-1}$]
τ_{wall} wall shear stress [pa]
u_j liquid velocity in stationary reference frame[$m\ s^{-1}$]
v_j velocity component arising from mesh motion[$m\ s^{-1}$]
p pressure [$N\ m^{-2}$]
τ_{ij} stress tensor[$kg\ m^{-1}\ s^{-2}$]

Parameter of Agitated vessel

B   width of baffles [m]
D   vessel diameter [m]
H   vessel height /Liquid height [m]
D   impeller diameter [m]
w   width of impeller blade [m]
h   height of impeller from bottom of agitated vessel [m]
h/d   off-bottom clearance [m]
t   bade thickness [m]
n_B number of blades
$\bar{\alpha}$ pitch angle of blade [^{0}]

B   number of baffles [-]
b_t baffle thickness [m]
N   impeller rotation speed [s^{-1}]
P   power [W
t_m run simulation time [s^{-1}]

Fluid properties

ρ density of fluid [Kg m^{-3}]
μ dynamic viscosity of the fluid [Pa.s]
Cp specific heat capacity of fluid [J kg^{-1} K^{-1}]
λ thermal conductivity [W m^{-1} K^{-1}]
ν kinematic viscosity [m^2 s^{-1}]

Heat transfer

A   heat transfer area [m^2]
q heat flux [W m^{-2}]
Q heat transfer rate [m^2]
α heat transfer coefficient [W m^{-2} K]
s haet transfer rate [W m^{-2} K]
T temperatue [K]
$\Delta\overline{T}$ mean temperature difference [K]
T_h temperature of the heating medium [K]
T_b temperature of batch liquid [K]
m mass of batch liquid [kg]
μ_b dynamic viscosity for the bulk of fluid [Pa.s]
μ_w dynamic viscosity of fluid at wall [Pa.s]
Δt heating time [s]
U overall heat transfer coefficient [W m^{-2} K^{-1}]
τ moment (torque)[N.m^{-1}]
ω angular velocity of impeller [rad s^{-1}]
t_m mixing time [s]
$\dot{q}^{(g)}$ heat source [J]
$\dot{Q}^{(g)}$ heat sink [J]
T_w temperature at the wall [K]
S   surface[m]
T_f final temperature[K]
V_{tank} volume of tank [m^3]
$\dfrac{d_R}{d_B}$ impeller diameter to vessel diameter [m]

APPENDIX

A) The 'nlinfit2' function written in MATLAB

```
function [ a, resid, Jc, ci, cip, cipp ] = nlinfit2(Xi,Yi,fmodel,Binit)
np = length(Binit);
if  (~ exist('OCTAVE_VERSION'))
[a,resid,Jc,covb] = nlinfit(Xi,Yi,fmodel,Binit);
ci = nlparci(a,resid,'jacobian',Jc,'alpha',1-0.95);
cip = a' - ci(:,1);
else
% leasqr in Octave expects opposite order of input parameters
fmodel2 = @(x,a) fmodel(a,x);
[y2,a,kvg,iter,corp,covp,covr,stdresid,Z,r2] = leasqr(Xi,Yi,Binit,fmodel2);%%beta
= a;
resid = Yi - y2; % residua
N = length(Xi);
nf = N-np;Sv2 = sum(resid.^2)/nf;
%covp
Jc = [];
C = sum(stdresid.^2)/nf*covp;
t975 = tinv(0.975,nf);
for i=1:np;
stde(i) = sqrt(C(i,i));
cip(i) = stde(i)*t975;
ci(i,:) = [a(i)-cip(i),a(i)+cip(i)];
end
end
cipp = cip./abs(a')*100;
for i=1:np;
fprintf('beta(%d): %12f +- %10f (%.2f%%),  %12f ...
%12f\n',i,a(i),cip(i),cipp(i),ci(i,:));
end
```

B) The MATLAB file for the functional relationship Power number Po vs Reynolds number Re described by null hypothesis.

```
Xi = [22116 36860 51604 66348 22116 29488 36860 44232 51604 58976 66348 22116 36860 51604 66348]
Yi = [1.62 1.61 1.79 2.01 1.76 1.66 1.88 1.88 1.88 1.83 1.87 1.62 1.61 1.79 2.01]
fmodel = @(b,x) b(1)*x.^b(2); %power model
[b,resid,J] = nlinfit2(Xi,Yi,fmodel,[1 1]);
b
SSalt = sum( resid.^2 )
N = length(Xi)
DFalt = N - 2
fmodel1 = @(b,x) b(1)*x.^0; %null hypothesis
[b0,resid0,J0] = nlinfit2(Xi,Yi,fmodel1,[1]);
b0
SSnull = sum( resid0.^2 )
DFnull = N - 1
F = ( (SSnull-SSalt)/SSalt )/( (DFnull-DFalt)/DFalt )
Fcrit = finv(0.95,DFnull-DFalt,DFalt)
Pr = fcdf(F,DFnull-DFalt,DFalt)
p = 1-Pr
if ( F < Fcrit )
disp('no significant difference');
else
disp('significant difference');
end
y1 = fmodel(b,Xi);
y0 = fmodel1(b0,Xi);
figure(4);
loglog(Xi,Yi,'r*', Xi,y1, Xi,y0);
axis([0.9*min(Xi), 1.1*max(Xi), 0.5, 3]);
grid on;
```

C) Calculation table for off -bottom clearance h/d=2/3

Heat flux (W/m^2)	N(RPM)	N(rps)	Angular velocity rad/s	Moment (n-m)	Power P (W)	Power number Po	Diameter of vessel (d)	Diameter of impeller (m)
3000	300	5.00	31.41	0.009	0.289	1.76	0.2	0.0667
3000	400	6.67	41.88	0.015	0.647	1.66	0.2	0.0667
3000	500	8.33	52.35	0.027	1.427	1.88	0.2	0.0667
30000	500	8.33	52.35	0.027	1.427	1.88	0.2	0.0667
3000	600	10.00	62.83	0.039	2.473	1.88	0.2	0.0667
3000	700	11.67	73.30	0.053	3.920	1.88	0.2	0.0667
3000	800	13.33	83.77	0.068	5.692	1.83	0.2	0.0667
3000	900	15.00	94.24	0.088	8.299	1.87	0.2	0.0667

dynamic viscosity (Pa.s)	Reynolds Number	mean alpha (w/m2-k)	mean alpha bottom	mean alpha wall	Mean Nusselt (bottom+ wall)	Mean Nusselt (Bottom)
0.0010	22116	2207.899	3382.499	1912.000	735.966	1127.500
0.0010	29488	2797.980	4226.677	2438.071	932.660	1408.892
0.0010	36860	3404.102	5101.563	2976.487	1134.701	1700.521
0.0010	36860	3404.082	5101.500	2976.477	1134.694	1700.500
0.0010	44232	3927.515	5802.120	3455.275	1309.172	1934.040
0.0010	51604	4644.879	6640.802	4142.077	1548.293	2213.601
0.0010	58976	5149.296	7389.914	4584.852	1716.432	2463.305
0.0010	66348	5860.863	8168.816	5279.456	1953.621	2722.939

Mean Nusselt (wall)	Prandlt Pr^(1/3)	Nusselt (Bottom +Wall) /Pr^(1/3)	Nusselt (bottom)/Pr^(1/3)	Nusselt(wall)/ Pr^(1/3)
637.333	1.912	384.889	589.665	333.315
812.690	1.912	487.767	736.829	425.024
992.162	1.912	593.431	889.346	518.885
992.159	1.912	593.427	889.335	518.884
1151.758	1.912	684.676	1011.473	602.352
1380.692	1.912	809.733	1157.679	722.081
1528.284	1.912	897.667	1288.270	799.269
1759.819	1.912	1021.713	1424.055	920.358

Calculation table for off-bottom clearance h/d = 1/3

N(RPM)	Angular velocity (rad/s)	Moment (n-m)	Power (P) W	Power number (Po)	Diameter of vessel (d)	Diameter of impeller (m)
300	31.4159	0.0110	0.347	2.11	0.20	0.0667
500	52.3599	0.0296	1.549	2.04	0.20	0.0667
700	73.3038	0.0569	4.174	2.00	0.20	0.0667
900	94.2478	0.1077	10.148	2.29	0.20	0.0667

Reynolds Number	Mean alpha (w/m2-k)	Mean alpha bottom	Mean alpha wall	Mean Nusselt (Bottom + wall)	Mean Nusselt (Bottom)	Mean Nusselt (wall)
22116	2582.866	3839.656	2266.263	860.955	1279.885	755.421
36860	3896.019	5764.561	3425.306	1298.673	1921.520	1141.769
51604	5156.916	7469.290	4574.396	1718.972	2489.763	1524.799
66348	6735.729	9083.646	6144.255	2245.243	3027.882	2048.085

Prandtl Pr^(1/3)	Nusselt (bottom+wall)/Pr(1/3)	Nusselt (bottom)/Pr^(1/3)	Nusselt (wall)/Pr^(1/3)
1.912	450.266	669.360	395.073
1.912	679.186	1004.925	597.127
1.912	898.996	1302.107	797.446
1.912	1174227	1583.535	1071.117

Calculation table for off-bottom clearance h/d= 1

Nusselt (Bottom+wall)/Pr^(1/3)	Nusselt (bottom)/Pr^(1/3)	Nusselt (wall)/Pr^(1/3)
345.541	474.903	312.954
498.156	705.687	445.876
685.612	954.338	617.916
882.382	1185.616	805.993

D) MATLAB script for h/d = 2/3 nonlinear regression and similar code is used for h/d= 1, h=/d1/3.

```matlab
clear all
clc
data = load('data_allc.csv')% only h/d = 2/3

disp('--- h/d = 2/3 ---');
Xi = data(1:7,2);
Yi = data(1:7,4);%./data(1:7,5);
fmodel = @(b,x) b(1)*x.^b(2);
[b,resid,J] = nlinfit2(Xi,Yi,fmodel,[1 1]);
x = linspace(min(Xi),max(Xi),30);
y = fmodel(b,x);
% Chapman correlation
Xi_1 = Xi;
Yi_1 = 0.53*Xi_1.^0.66;
dr=66.6667;
db=200;
h=20;
hr=44.44; % off-bottom clearnce 1/3
hl=200;
thita=45;
z=6;
dv=1;
dvw=1;
Xi_2 = Xi;
Yi_2 = 1.4.*((dr./db).^(-0.3)).*((h ./db).^(0.45)).*((hr./hl).^(0.2)).*((hl./db).^(-0.6)).*(sind(thita).^(0.5)).*(z.^(0.2)).*(Xi_2.^(2/3)).* ((dv./dvw).^(0.14))
figure(1);
loglog(Xi,Yi,'bsq', x,y,'b-')
hold on;
loglog(Xi_1,Yi_1,'r-')
loglog(Xi_2,Yi_2,'g-')
xlabel('Re')
ylabel('Nu / (Pr^1/3)')
legend('fluent data','regression','Chapman','Nagata')
title('Re vs Nu / Pr^1/3')
hold off
axis([20000 70000 100 1000]);
grid on
% table
disp('values form fluent')
t1=table(Xi,Yi)
disp('values calculated from chapman')
t2=table(Xi_1,Yi_1)
```

E) MATLAB script for h/d = 2/3 nonlinear regression with the parameter *C* in the correlation coefficients for Nusselt number with fixed of exponent of Reynolds number used 0.66 case off-bottom clearance h/d = 2/3.

```
data = load('data_allc.csv');
size(data)
Xi = data(1:7,2);
Yi = data(1:7,4);
Pr = 7.021;
fmodel = @(b,x) b(1)*x.^(2/3);  %*Pr^(1/3);
fmodel2 = @(b,x) b(1)*x.^b(2); %*Pr^(1/3);
[b,resid,J] = nlinfit2(Xi,Yi,fmodel,[1]);
[b2,resid2,J2] = nlinfit2(Xi,Yi,fmodel2,[1 1]);
x = linspace(min(Xi),max(Xi),30);
y = fmodel(b,x);
y2 = fmodel2(b2,x);
loglog(Xi,Yi,'r*', x,y,'b-', x,y2,'g-');
```